US 20250268110A1

(19) **United States**

(12) **Patent Application Publication** (10) **Pub. No.: US 2025/0268110 A1**

LE et al. (43) **Pub. Date: Aug. 21, 2025**

(54) **IMPROVED YPTBI COMPOSITION IN SPIN ORBIT TORQUE DEVICES**

(71) Applicants: **Western Digital Technologies, Inc.**, San Jose, CA (US); **INSTITUTE OF SCIENCE TOKYO**, Tokyo (JP)

(72) Inventors: **Quang LE**, San Jose, CA (US); **Maki MAEDA**, Fujisawa-shi, Kanagawa (JP); **Sho KAGAMI**, Yokohama (JP); **Nam Hai PHAM**, Tokyo (JP)

(73) Assignee: **Western Digital Technologies, Inc.**, San Jose, CA (US)

(21) Appl. No.: **19/067,574**

(22) Filed: **Feb. 28, 2025**

Related U.S. Application Data

(63) Continuation-in-part of application No. 19/011,206, filed on Jan. 6, 2025.

(60) Provisional application No. 63/554,533, filed on Feb. 16, 2024.

Publication Classification

(51) **Int. Cl.**

H10N 50/85	(2023.01)
G11B 5/00	(2006.01)
G11B 5/39	(2006.01)
G11C 11/16	(2006.01)
H10N 50/10	(2023.01)
H10N 52/80	(2023.01)

(52) **U.S. Cl.**

CPC ***H10N 50/85*** (2023.02); ***G11B 5/3909*** (2013.01); ***G11C 11/161*** (2013.01); ***H10N 50/10*** (2023.02); ***H10N 52/80*** (2023.02); *G11B 2005/0024* (2013.01)

(57) **ABSTRACT**

The present disclosure generally relates to topological semimetal (TSM) based spin-orbit torque (SOT) devices, and methods of forming a TSM layer. The TSM layer of the SOT device comprises YPtBi having a 1:1.02:1.05 stoichiometry to a 1:1.25:1.35 stoichiometry, such as a 1:1.11:1.13 stoichiometry. The TSM layer comprising about 10% less of Y compared to Pt and Bi increases the spin Hall angle (SHA) and the spin Hall conductivity. Increasing the Pt concentration ratio to greater than 1 enhances both the SHA and the spin Hall conductivity of the TSM layer by a factor of two, and further helps increase the YPtBi surface grain size, which in turn helps improve the interface spin transparency. Increasing the Bi/Y concentration ratio to greater than 1 approaching that of Pt enhances both the resistivity of the TSM layer and the effective SHA by a factor of two.

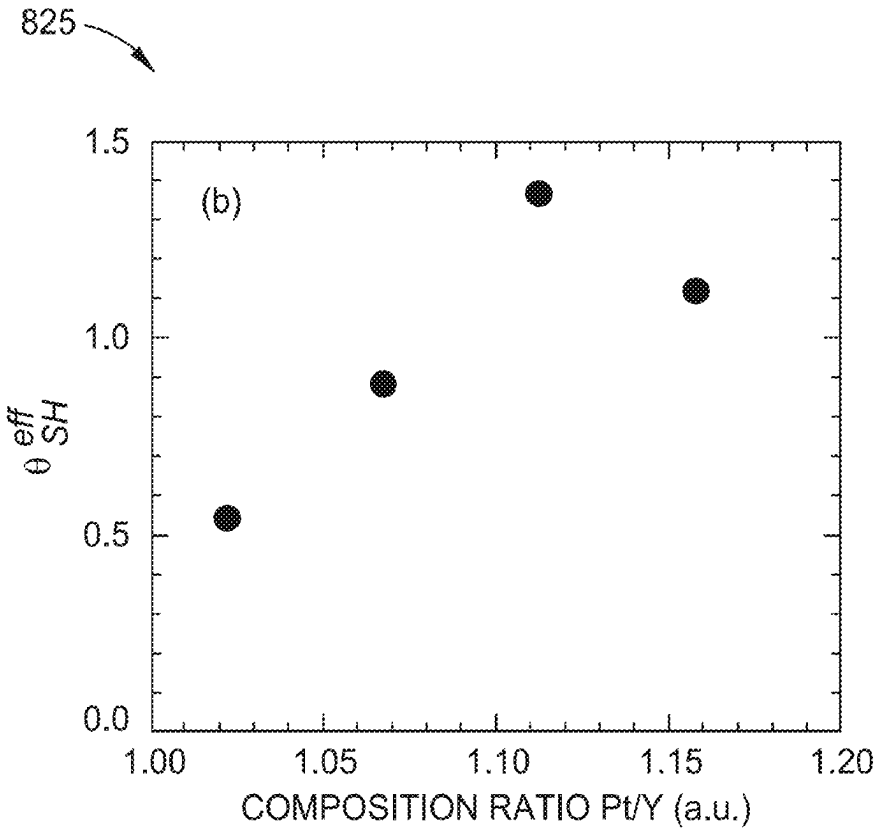

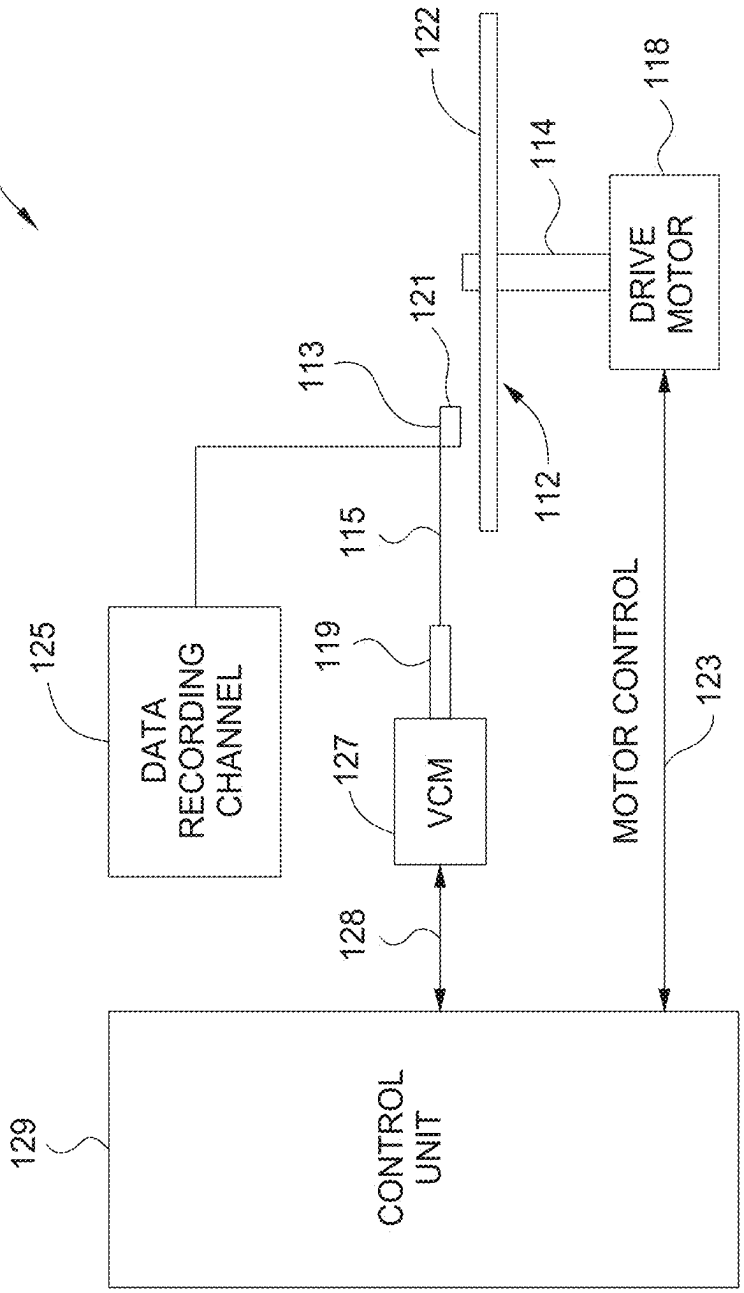
100
122
118
114
DRIVE MOTOR
121
113
112
115
125
DATA RECORDING CHANNEL
119
127
VCM
MOTOR CONTROL
123
128
129
CONTROL UNIT

FIG. 1

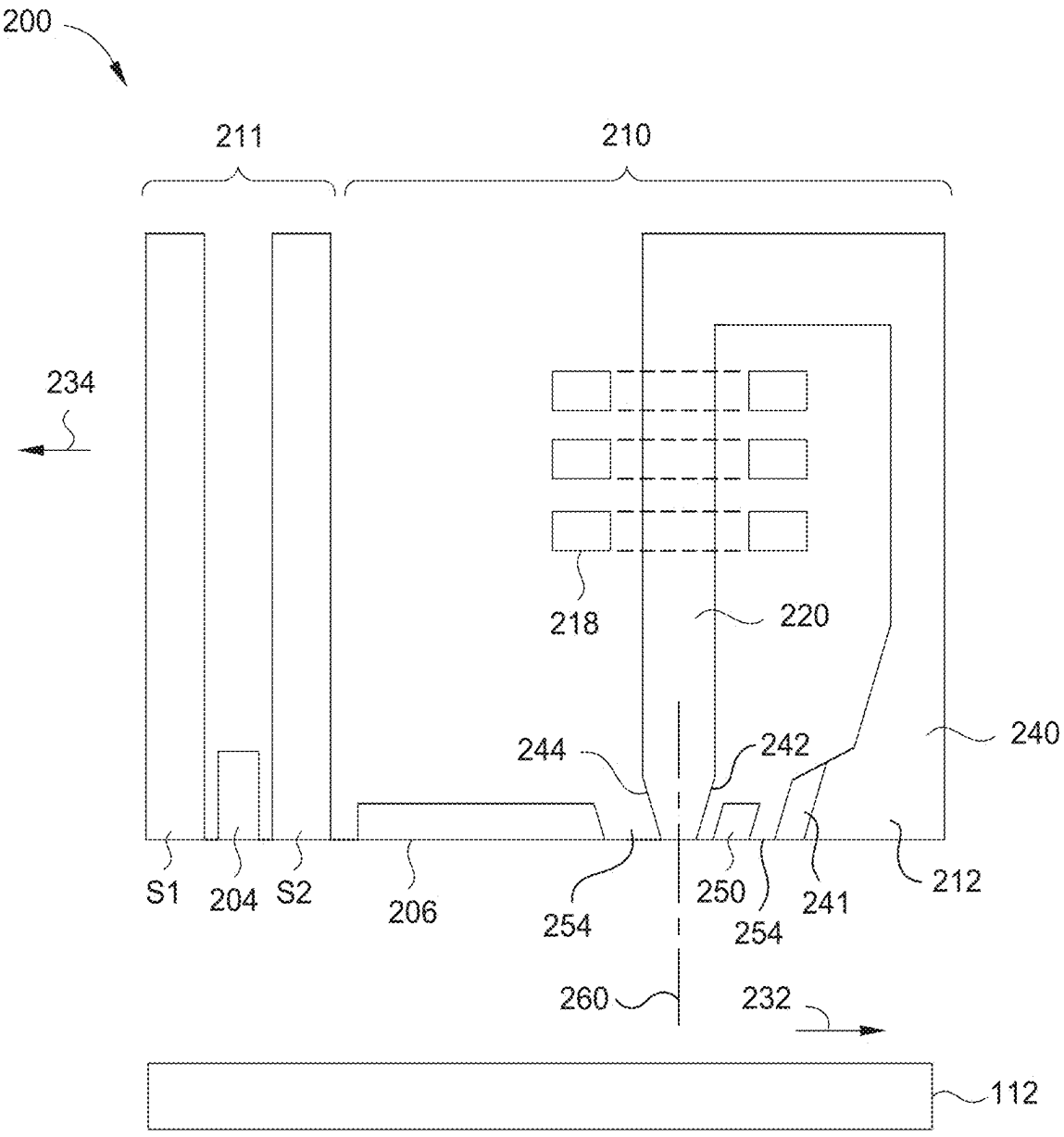
200
211
210
234
218
220
240
244
242
S1
204
S2
206
254
250
254
241
212
260
232
112

FIG. 2

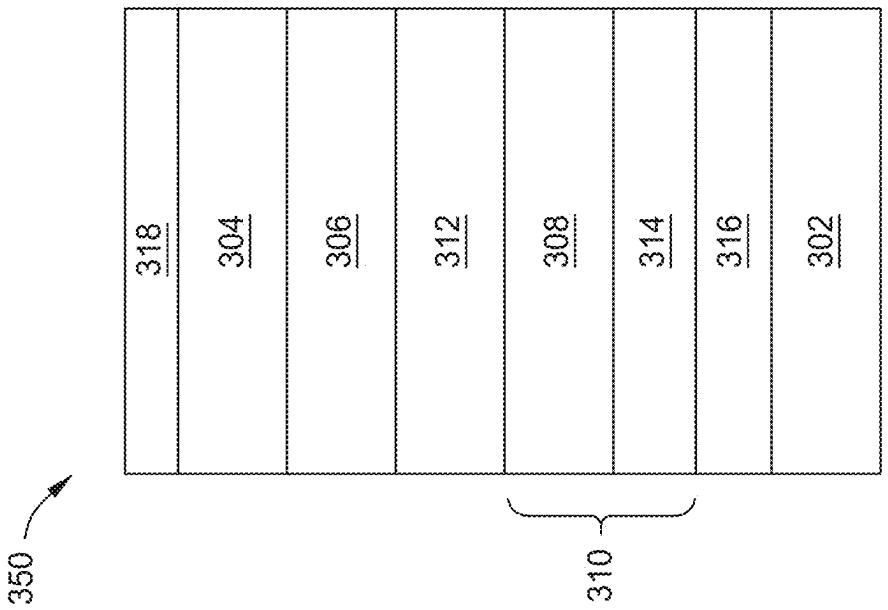
350
318
304
306
312
308
314
316
302
310
X
Y
Z

FIG. 3B

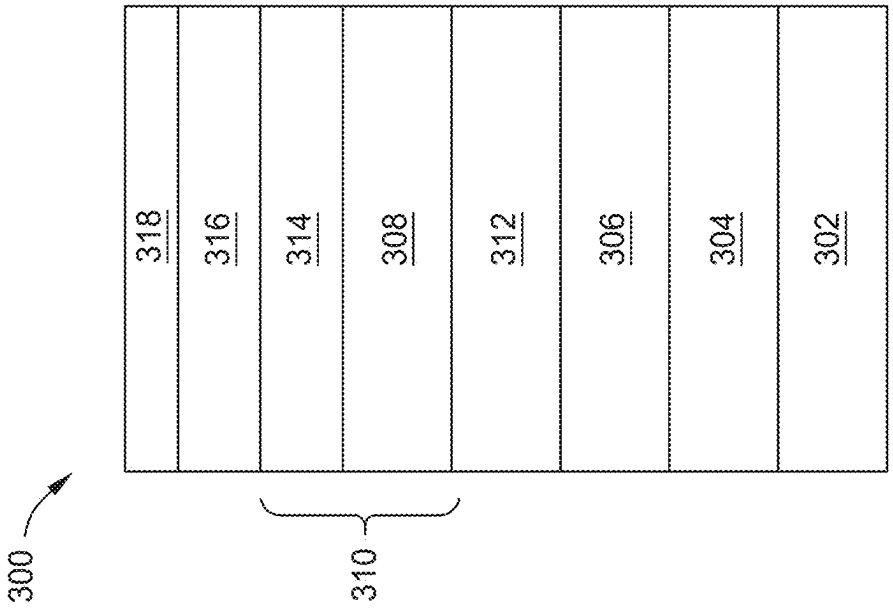
300
318
316
314
308
312
306
304
302
310

FIG. 3A

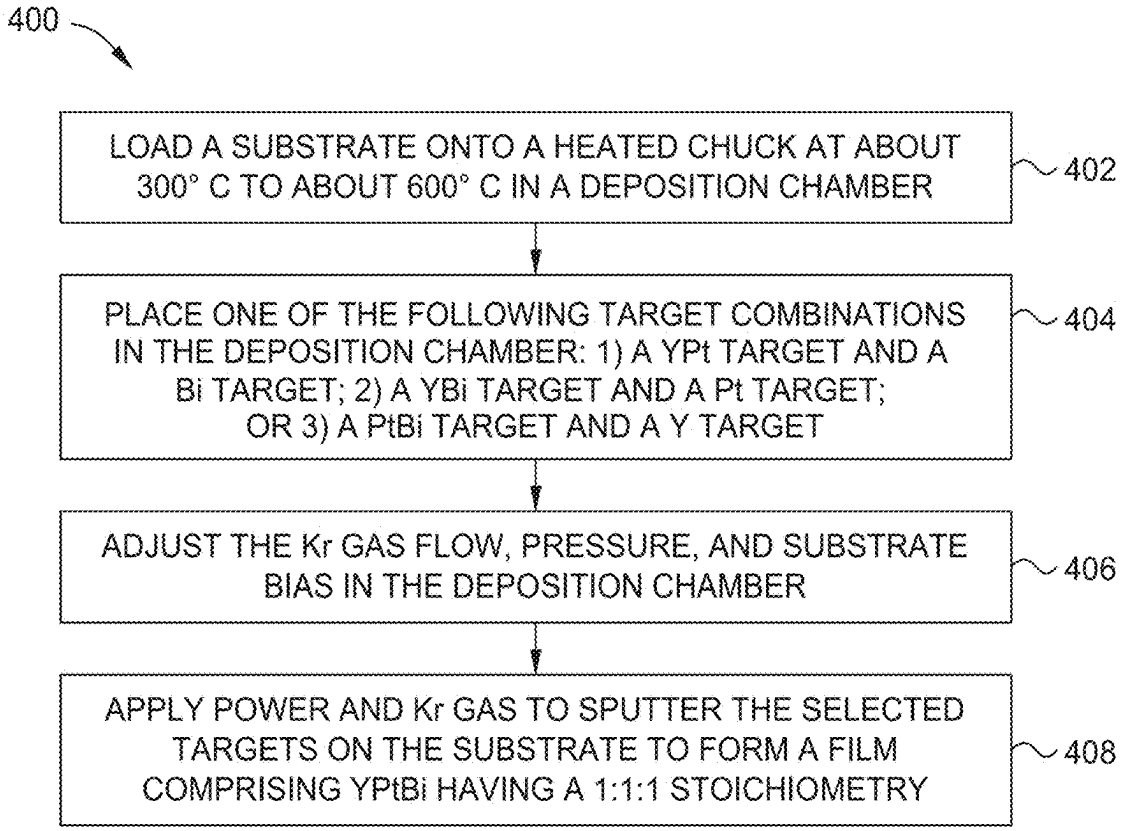
400
LOAD A SUBSTRATE ONTO A HEATED CHUCK AT ABOUT 300° C TO ABOUT 600° C IN A DEPOSITION CHAMBER
402
PLACE ONE OF THE FOLLOWING TARGET COMBINATIONS IN THE DEPOSITION CHAMBER: 1) A YPt TARGET AND A Bi TARGET; 2) A YBi TARGET AND A Pt TARGET; OR 3) A PtBi TARGET AND A Y TARGET
404
ADJUST THE Kr GAS FLOW, PRESSURE, AND SUBSTRATE BIAS IN THE DEPOSITION CHAMBER
406
APPLY POWER AND Kr GAS TO SPUTTER THE SELECTED TARGETS ON THE SUBSTRATE TO FORM A FILM COMPRISING YPtBi HAVING A 1:1:1 STOICHIOMETRY
408

FIG. 4A

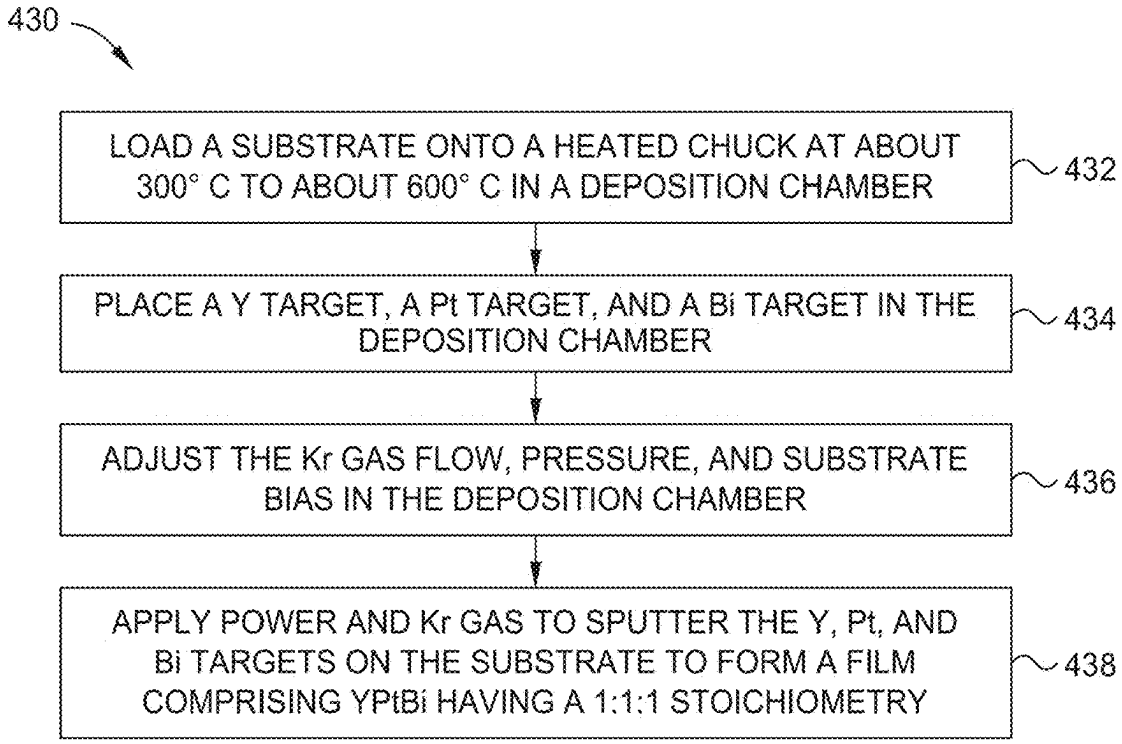
430
LOAD A SUBSTRATE ONTO A HEATED CHUCK AT ABOUT 300° C TO ABOUT 600° C IN A DEPOSITION CHAMBER
432
PLACE A Y TARGET, A Pt TARGET, AND A Bi TARGET IN THE DEPOSITION CHAMBER
434
ADJUST THE Kr GAS FLOW, PRESSURE, AND SUBSTRATE BIAS IN THE DEPOSITION CHAMBER
436
APPLY POWER AND Kr GAS TO SPUTTER THE Y, Pt, AND Bi TARGETS ON THE SUBSTRATE TO FORM A FILM COMPRISING YPtBi HAVING A 1:1:1 STOICHIOMETRY
438

FIG. 4B

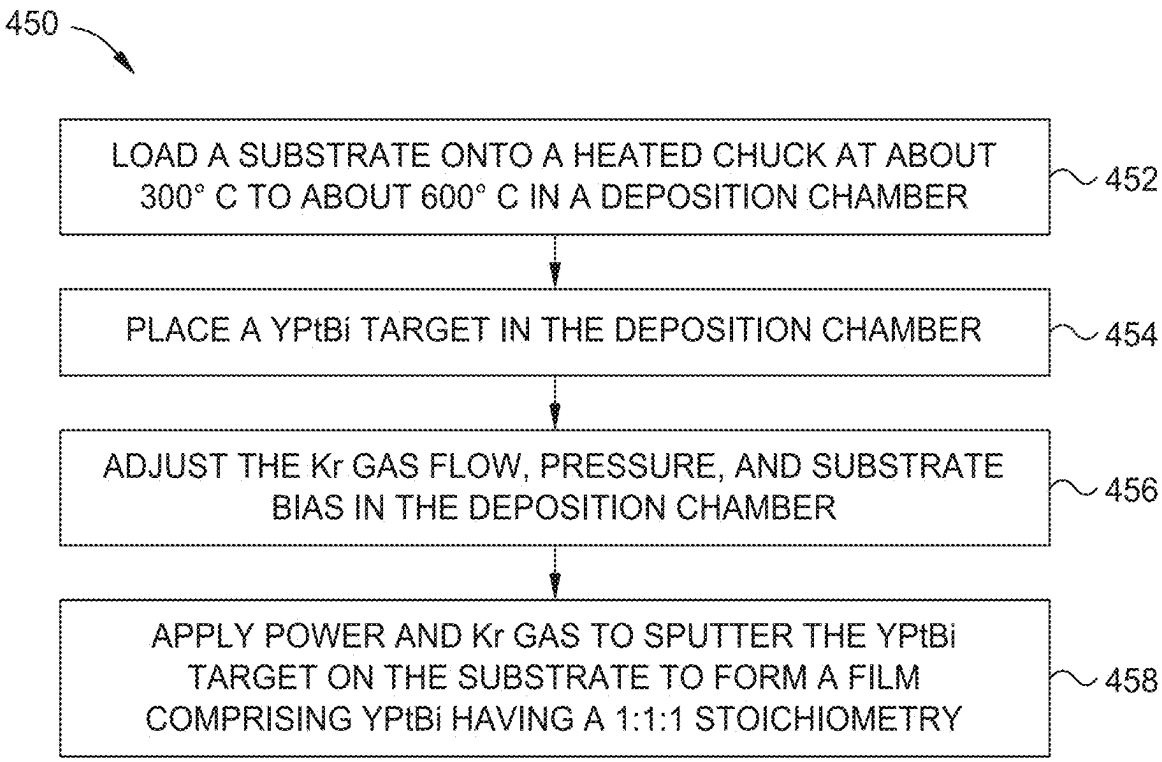
450
LOAD A SUBSTRATE ONTO A HEATED CHUCK AT ABOUT 300° C TO ABOUT 600° C IN A DEPOSITION CHAMBER
452
PLACE A YPtBi TARGET IN THE DEPOSITION CHAMBER
454
ADJUST THE Kr GAS FLOW, PRESSURE, AND SUBSTRATE BIAS IN THE DEPOSITION CHAMBER
456
APPLY POWER AND Kr GAS TO SPUTTER THE YPtBi TARGET ON THE SUBSTRATE TO FORM A FILM COMPRISING YPtBi HAVING A 1:1:1 STOICHIOMETRY
458

FIG. 4C

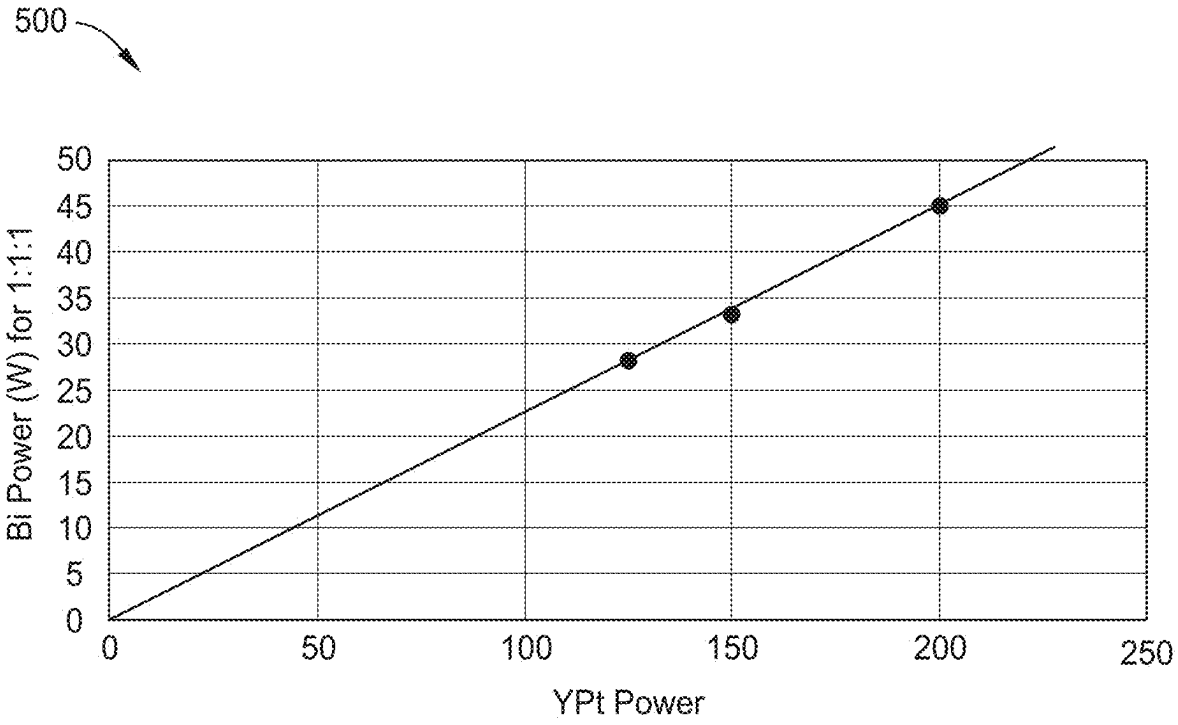
500
Bi Power (W) for 1:1:1
50
45
40
35
30
25
20
15
10
5
0
0
50
100
150
200
250
YPt Power

FIG. 5A

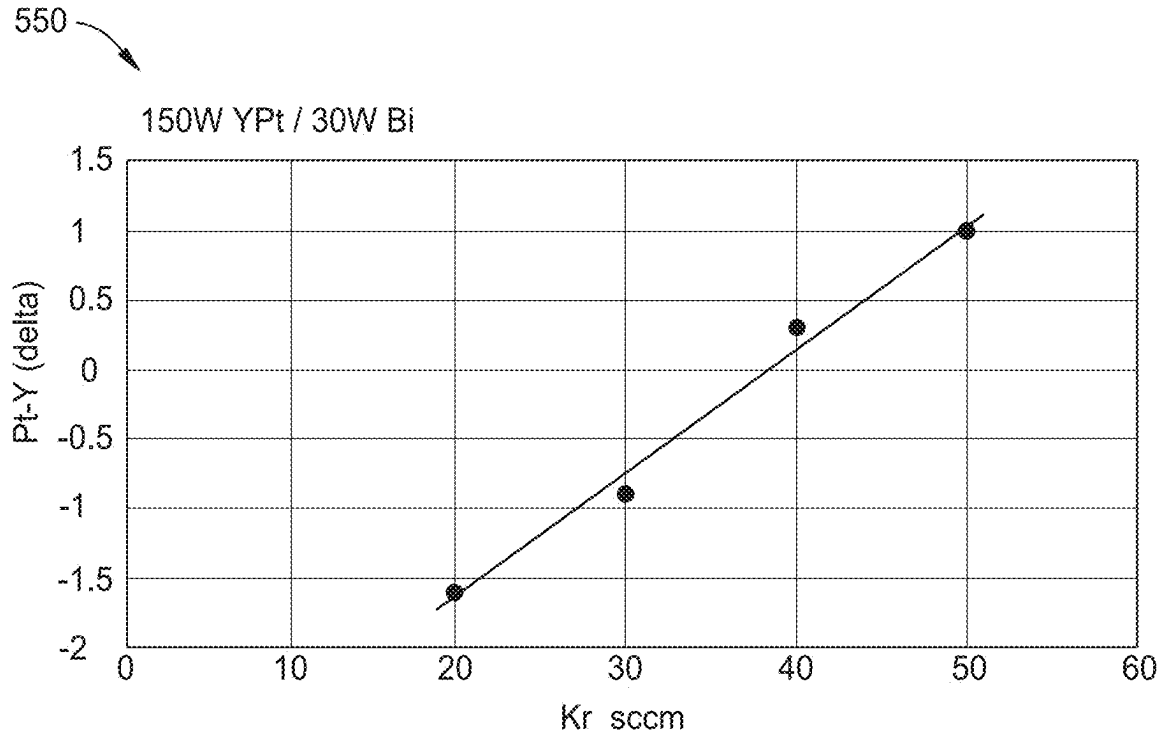
550
150W YPt / 30W Bi
Pt-Y (delta)
1.5
1
0.5
0
-0.5
-1
-1.5
-2
0
10
20
30
40
50
60
Kr sccm

FIG. 5B

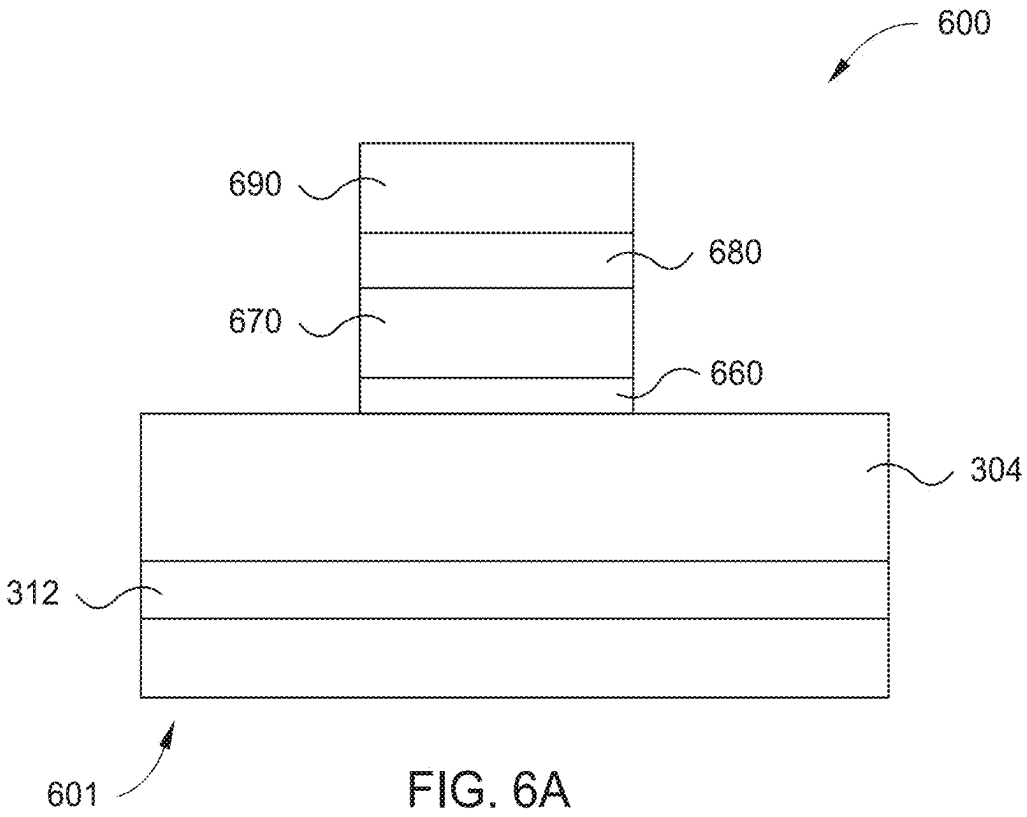

FIG. 6A

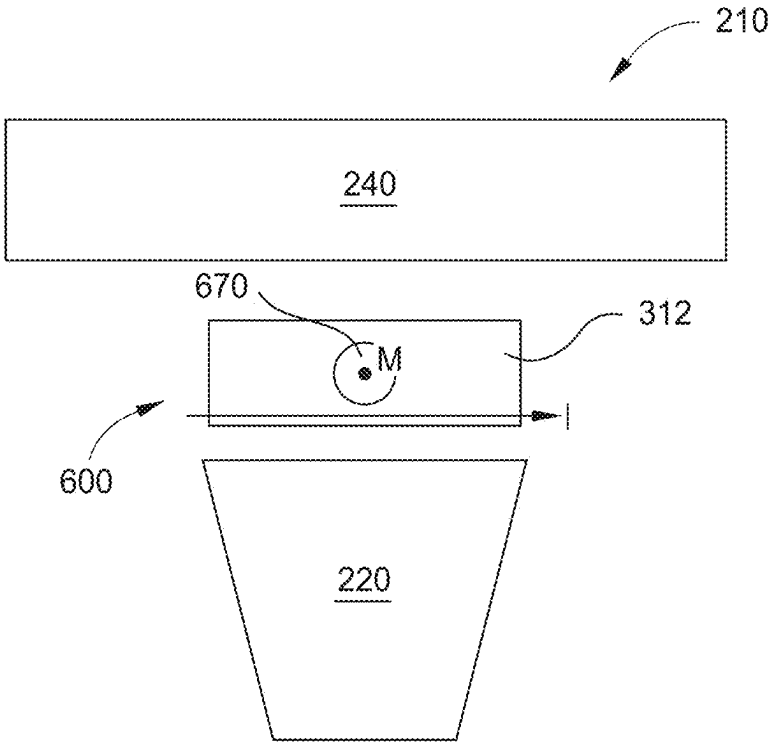

FIG. 6B

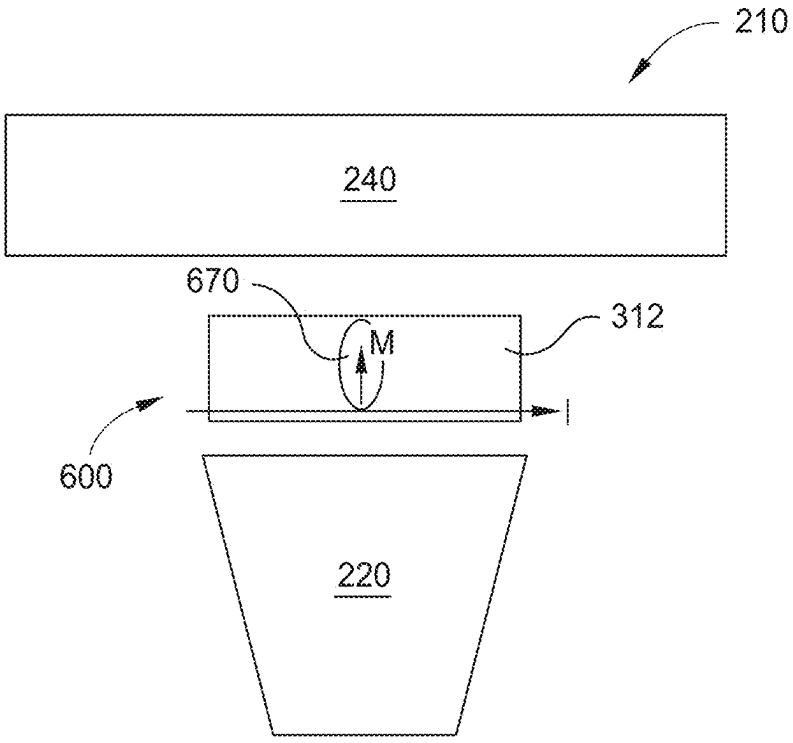

FIG. 6C

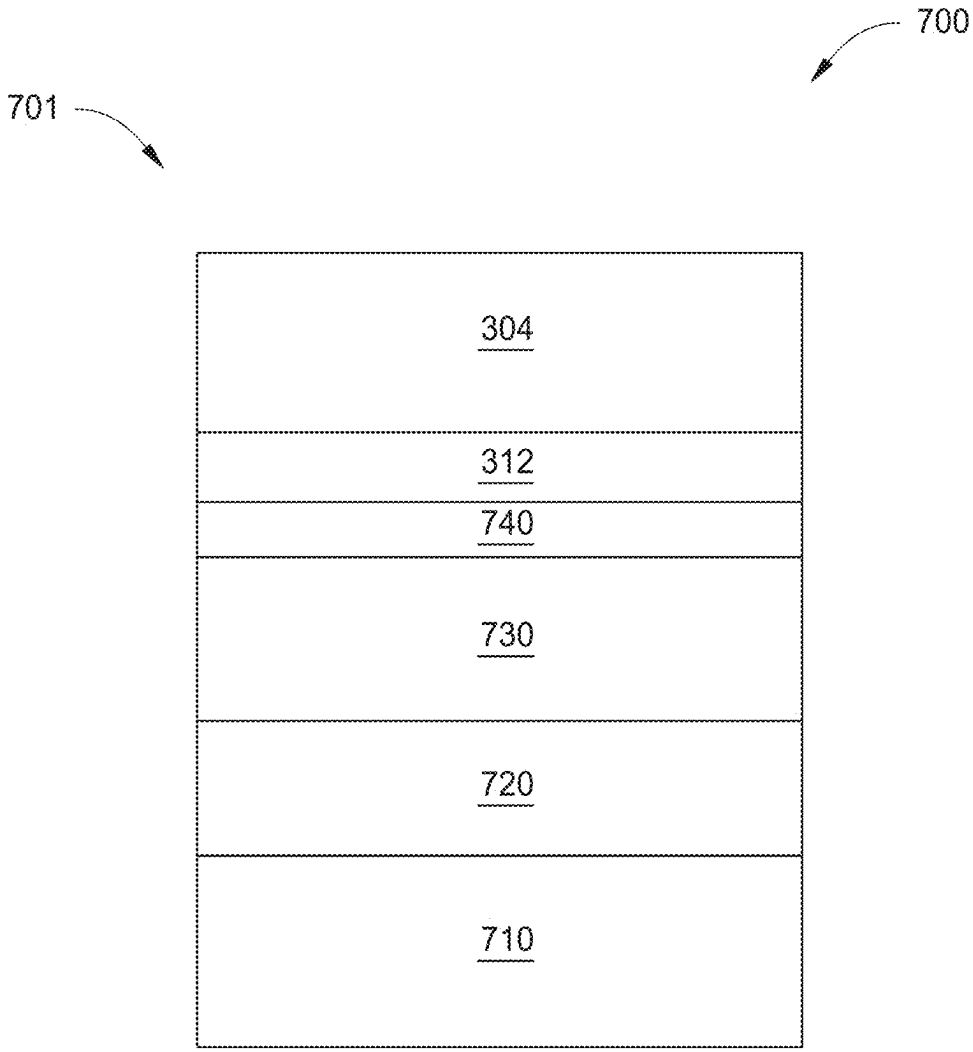

FIG. 7

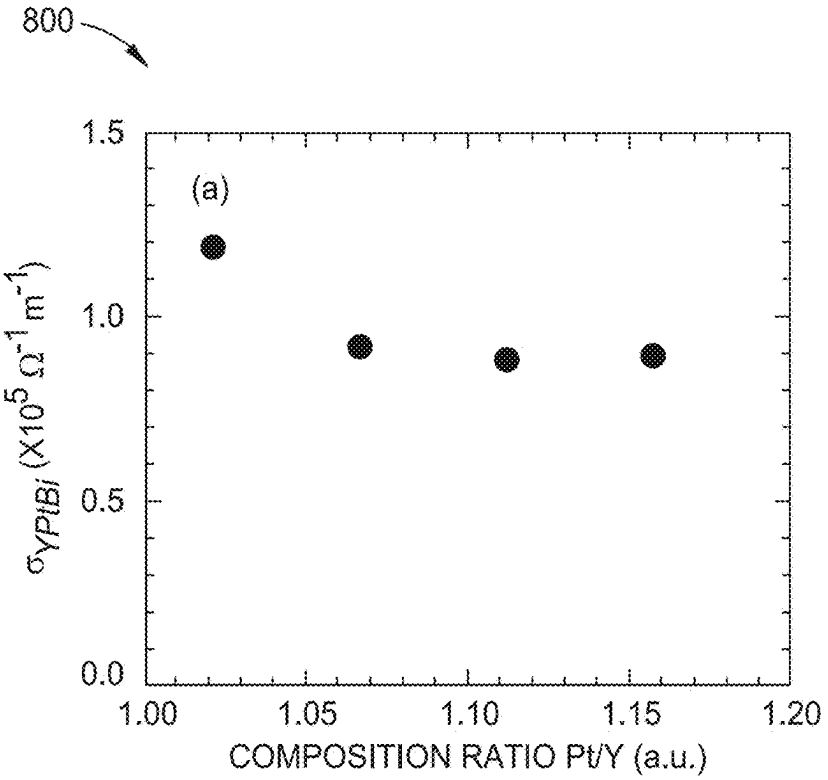
800
(a)
1.5
1.0
0.5
0.0
σ_{YPtBi} (X10^5 Ω^{-1} m^{-1})
1.00
1.05
1.10
1.15
1.20
COMPOSITION RATIO Pt/Y (a.u.)

FIG. 8A

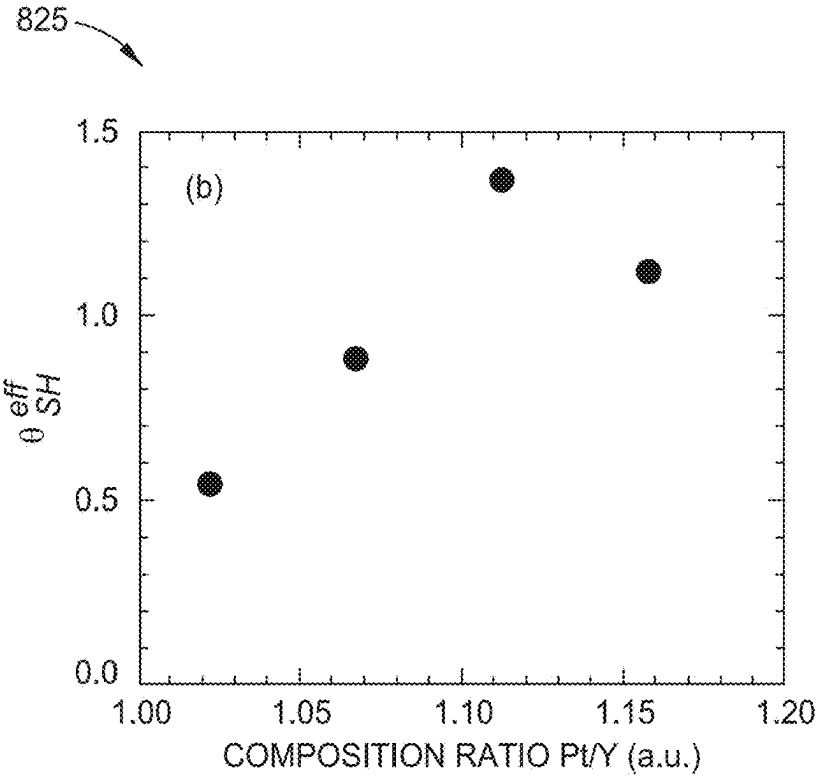
825
(b)
1.5
1.0
0.5
0.0
θ_{SH}^{eff}
1.00
1.05
1.10
1.15
1.20
COMPOSITION RATIO Pt/Y (a.u.)

FIG. 8B

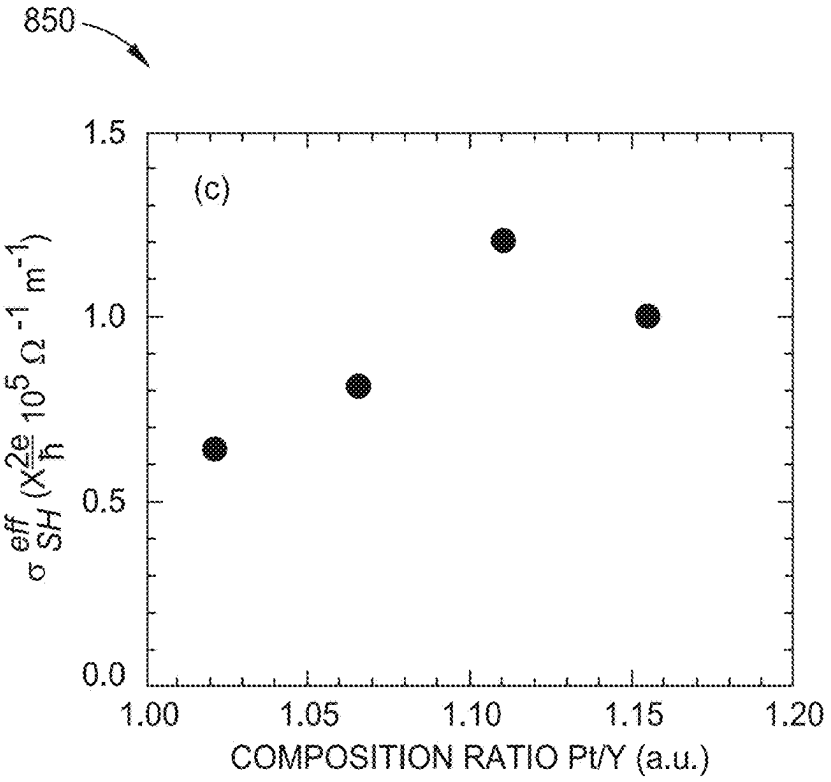
850
(c)
1.5
1.0
0.5
0.0
1.00
1.05
1.10
1.15
1.20
COMPOSITION RATIO Pt/Y (a.u.)
σ SH eff (X 2e/h 10^5 Ω^-1 m^-1)

FIG. 8C

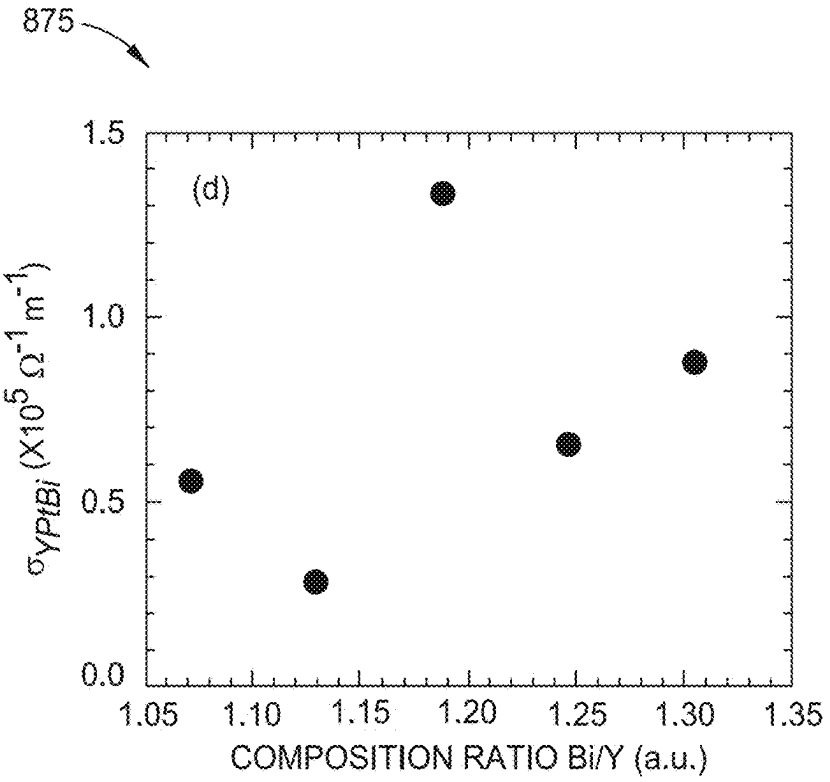
875
(d)
1.5
1.0
0.5
0.0
1.05
1.10
1.15
1.20
1.25
1.30
1.35
COMPOSITION RATIO Bi/Y (a.u.)
σYPtBi (X10^5 Ω^-1 m^-1)

FIG. 8D

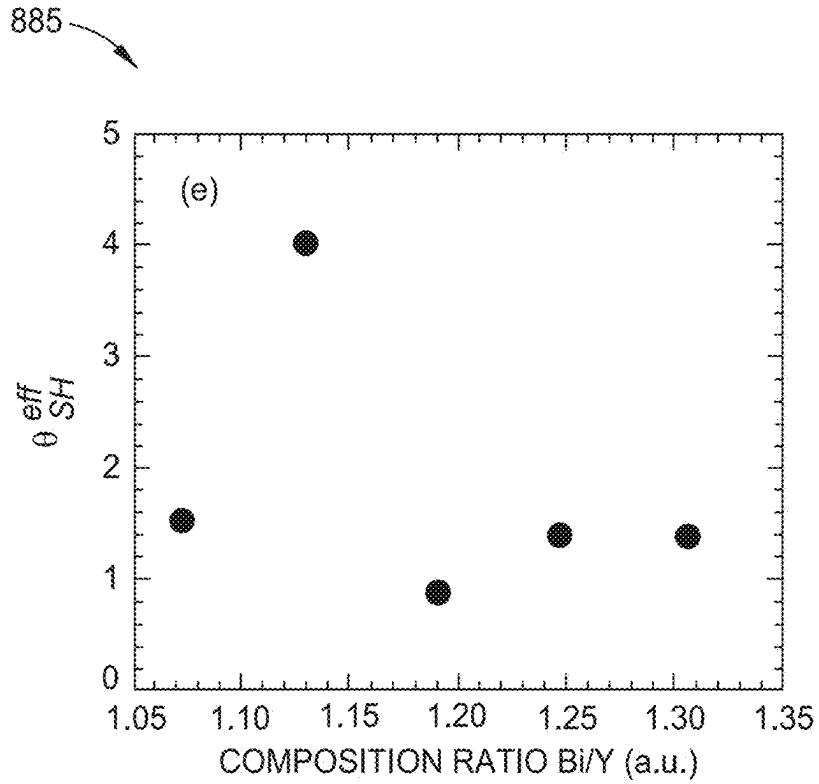
885
(e)
θ_{SH}^{eff}
5
4
3
2
1
0
1.05
1.10
1.15
1.20
1.25
1.30
1.35
COMPOSITION RATIO Bi/Y (a.u.)

FIG. 8E

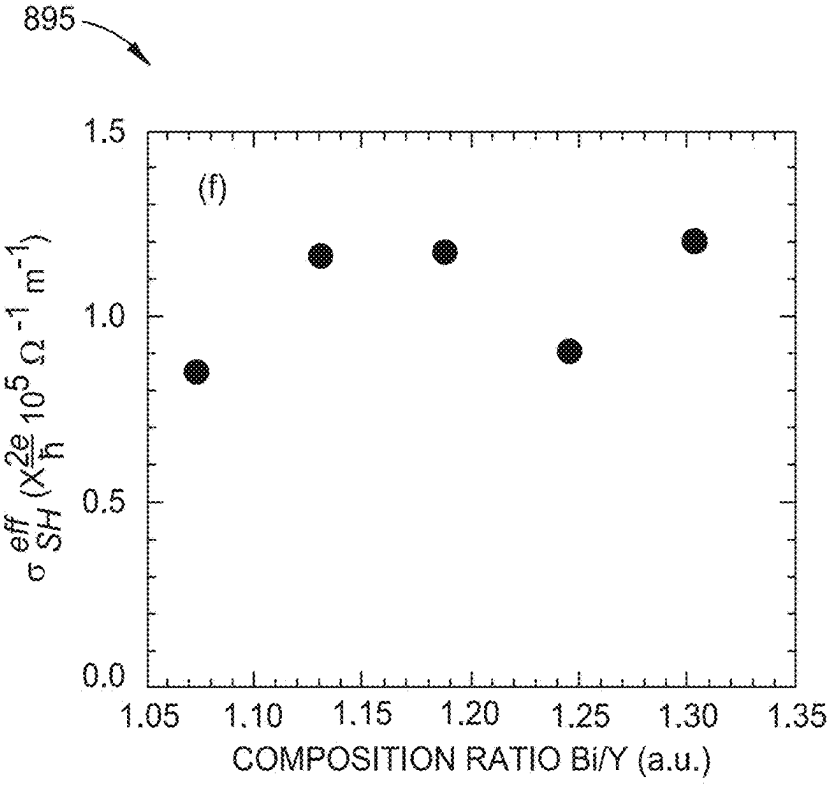
895
(f)
$\sigma_{SH}^{eff}(X\frac{2e}{h}10^5\ \Omega^{-1}\ m^{-1})$
1.5
1.0
0.5
0.0
1.05
1.10
1.15
1.20
1.25
1.30
1.35
COMPOSITION RATIO Bi/Y (a.u.)

FIG. 8F

IMPROVED YPTBI COMPOSITION IN SPIN ORBIT TORQUE DEVICES

CROSS-REFERENCE TO RELATED APPLICATIONS

[0001] This application is a continuation-in-part of co-pending U.S. patent application Ser. No. 19/011,206, filed Jan. 6, 2025, which claims benefit of U.S. provisional patent application Ser. No. 63/554,533, filed Feb. 16, 2024, each of which is herein incorporated by reference.

BACKGROUND OF THE DISCLOSURE

Field of the Disclosure

[0002] Embodiments of the present disclosure generally relate to spin-orbit torque (SOT) device comprising a topological semi-metal (TSM) layer.

Description of the Related Art

[0003] YPtBi layers are zero band gap topological semimetals having both giant spin Hall effect and high electrical conductivity. YPtBi is a material that has been proposed in various spin-orbit torque (SOT) device applications, such as for a spin Hall layer for magnetoresistive random access memory (MRAM) devices, magnetic recording read heads, sensors, and energy-assisted magnetic recording (EAMR) magnetic recording heads. However, utilizing YPtBi materials in commercial SOT applications can present several obstacles. For example, YPtBi materials require specific buffer layers and/or interlayers, as well as optimal processing conditions, to achieve the desired orientation.

[0004] Therefore, there is a need for an improved SOT device utilizing TSM layer(s) having a desired crystal orientation.

SUMMARY OF THE DISCLOSURE

[0005] The present disclosure generally relates to topological semi-metal (TSM) based spin-orbit torque (SOT) devices, and methods of forming a TSM layer. The TSM layer of the SOT device comprises YPtBi having a 1:1.02:1.05 stoichiometry to a 1:1.25:1.35 stoichiometry, such as a 1:1.11:1.13 stoichiometry. The TSM layer comprising about 10% less of Y compared to Pt and Bi increases the spin Hall angle (SHA) and the spin Hall conductivity. Increasing the Pt concentration ratio to greater than 1 enhances both the SHA and the spin Hall conductivity by a factor of two, and further helps increase the YPtBi surface grain size, which in turn helps improve the interface spin transparency. Increasing the Bi/Y concentration ratio to greater than 1 approaching that of Pt enhances both the resistivity of the TSM layer and the effective SHA (θ_{SH}^{eff}) by a factor of two.

[0006] In one embodiment, a spin-orbit torque (SOT) device comprises a YPtBi layer having a 1:1.02:1.05 stoichiometry to a 1:1.25:1.35 stoichiometry.

[0007] In another embodiment, a spin-orbit torque (SOT) device comprises a YPtBi layer, wherein a concentration of Pt and Bi is about 10% greater than a concentration of Y.

[0008] In yet another embodiment, a spin-orbit torque (SOT) device comprises a YPtBi layer having a 1:1.02:1.05 stoichiometry to a 1:1.25:1.35 stoichiometry, wherein the YPtBi layer has a (100), (111), or (110) orientation, and a buffer layer disposed adjacent to the YPtBi layer.

BRIEF DESCRIPTION OF THE DRAWINGS

[0009] So that the manner in which the above-recited features of the present disclosure can be understood in detail, a more particular description of the disclosure, briefly summarized above, may be had by reference to embodiments, some of which are illustrated in the appended drawings. It is to be noted, however, that the appended drawings illustrate only typical embodiments of this disclosure and are therefore not to be considered limiting of its scope, for the disclosure may admit to other equally effective embodiments.

[0010] FIG. **1** is a schematic illustration of certain embodiments of a magnetic media drive including a magnetic recording head with a SOT MTJ device.

[0011] FIG. **2** is a fragmented, cross-sectional view of certain embodiments of a read/write head with a SOT MTJ device.

[0012] FIGS. **3**A-**3**B illustrate spin-orbit torque (SOT) devices, according to various embodiments.

[0013] FIGS. **4**A-**4**C illustrate methods of forming YPtBi having a 1:1:1 composition, according to various embodiments.

[0014] FIG. **5**A illustrates a graph showing the power (W) applied to the Bi target versus the power (W) applied to the YPt target, according to one embodiment.

[0015] FIG. **5**B illustrates a graph showing the stoichiometry of YPt versus Kr gas flow (sccm), according to one embodiment.

[0016] FIG. **6**A is a schematic cross-sectional view of a SOT device for use in a MAMR magnetic recording head, such as the MAMR magnetic recording head of the drive of FIG. **1** or other suitable magnetic media drives.

[0017] FIGS. **6**B-**6**C are schematic MFS views of certain embodiments of a portion of a MAMR magnetic recording head with a SOT device of FIG. **6**A.

[0018] FIG. **7** is a schematic cross-sectional view of a SOT MTJ used as a MRAM device.

[0019] FIG. **8**A illustrates a graph showing how the conductivity (σ_{YPtBi}) of the TSM layer is impacted when the composition ratio of Pt to Y (Pt/Y) in YPtBi is increased, according to one embodiment.

[0020] FIG. **8**B illustrates a graph showing how the effective spin Hall angle (θ_{SH}^{eff}) is impacted when the composition ratio of Pt to Y (Pt/Y) in YPtBi is increased, according to one embodiment.

[0021] FIG. **8**C illustrates a graph showing how the effective spin Hall conductivity (σ_{SH}^{eff}) is impacted when the composition ratio of Pt to Y (Pt/Y) in YPtBi is increased, according to one embodiment.

[0022] FIG. **8**D illustrates a graph showing how the conductivity (σ_{YPtBi}) of the TSM layer is impacted when the composition ratio of Bi to Y (Bi/Y) in YPtBi is increased, according to one embodiment.

[0023] FIG. **8**E illustrates a graph showing how the effective spin Hall angle (θ_{SH}^{eff}) is impacted when the composition ratio of Bi to Y (Bi/Y) in YPtBi is increased, according to another embodiment.

[0024] FIG. **8**F illustrates a graph showing how the effective spin Hall conductivity (σ_{SH}^{eff}) is impacted when the composition ratio of Bi to Y (Bi/Y) in YPtBi is increased, according to another embodiment.

[0025] To facilitate understanding, identical reference numerals have been used, where possible, to designate identical elements that are common to the figures. It is

contemplated that elements disclosed in one embodiment may be beneficially utilized on other embodiments without specific recitation.

DETAILED DESCRIPTION

[0026] In the following, reference is made to embodiments of the disclosure. However, it should be understood that the disclosure is not limited to specific described embodiments. Instead, any combination of the following features and elements, whether related to different embodiments or not, is contemplated to implement and practice the disclosure. Furthermore, although embodiments of the disclosure may achieve advantages over other possible solutions and/or the prior art, whether or not a given embodiment achieves a particular advantage is not limiting of the disclosure. Thus, the following aspects, features, embodiments, and benefits are merely illustrative and are not considered elements or limitations of the appended claims except where explicitly recited in a claim(s). Likewise, reference to "the disclosure" shall not be construed as a generalization of any inventive subject matter disclosed herein and shall not be considered to be an element or limitation of the appended claims except where explicitly recited in a claim(s).

[0027] The present disclosure generally relates to topological semi-metal (TSM) based spin-orbit torque (SOT) devices, and methods of forming a TSM layer. The TSM layer of the SOT device comprises YPtBi having a 1:1.02:1.05 stoichiometry to a 1:1.25:1.35 stoichiometry, such as a 1:1.11:1.13 stoichiometry. The TSM layer comprising about 10% less of Y compared to Pt and Bi increases the spin Hall angle (SHA) and the spin Hall conductivity. Increasing the Pt concentration ratio to greater than 1 enhances both the SHA and the spin Hall conductivity by a factor of two, and further helps increase the YPtBi surface grain size, which in turn helps improve the interface spin transparency. Increasing the Bi/Y concentration ratio to greater than 1 approaching that of Pt enhances both the resistivity of the TSM layer and the effective SHA (θ_{SH}^{eff}) by a factor of two.

[0028] FIG. **1** is a schematic illustration of certain embodiments of a magnetic media drive **100** including a magnetic recording head with a SOT MTJ device. Such a magnetic media drive may be a single drive or comprise multiple drives. For illustration, a single disk drive **100** is shown according to certain embodiments. As shown, at least one rotatable magnetic disk **112** is supported on a spindle **114** and rotated by a drive motor **118**. The magnetic recording on each magnetic disk **112** is in the form of any suitable patterns of data tracks, such as annular patterns of concentric data tracks (not shown) on the magnetic disk **112**.

[0029] At least one slider **113** is positioned near the magnetic disk **112**, and each slider **113** supports one or more magnetic head assemblies **121**, including a SOT device. As the magnetic disk **112** rotates, the slider **113** moves radially in and out over the disk surface **122** so that the magnetic head assembly **121** may access different tracks of the magnetic disk **112** where desired data are written. Each slider **113** is attached to an actuator arm **119** by a suspension **115**. The suspension **115** provides a slight spring force which biases the slider **113** toward the disk surface **122**. Each actuator arm **119** is attached to an actuator means **127**. The actuator means **127**, as shown in FIG. **2**, may be a voice coil motor (VCM). The VCM includes a coil movable within a fixed magnetic field, the direction and speed of the coil movements being controlled by the motor current signals supplied by the control unit **129**.

[0030] During operation of the disk drive **100**, the rotation of the magnetic disk **112** generates an air bearing between the slider **113** and the disk surface **122** which exerts an upward force or lift on the slider **113**. The air bearing thus counterbalances the slight spring force of suspension **115**, and supports slider **113** off and slightly above the disk surface **122** by a small, substantially constant spacing during regular operation.

[0031] The various components of the disk drive **100** are operated by control signals generated by control unit **129**, such as access control signals and internal clock signals. The control unit **129** typically comprises logic control circuits, storage means, and a microprocessor. The control unit **129** generates control signals to control various system operations such as drive motor control signals on line **123** and head position and seek control signals on line **128**. The control signals on line **128** provide the desired current profiles to move optimally and position slider **113** to the desired data track on disk **112**. Write and read signals are communicated to and from write and read heads on the assembly **121** by recording channel **125**.

[0032] The above description of a typical magnetic media drive and the accompanying illustration of FIG. **1** are for representation purposes only. It should be apparent that magnetic media drives may contain a large number of media, or disks, and actuators, and each actuator may support a number of sliders.

[0033] FIG. **2** is a fragmented, cross-sectional side view of certain embodiments of a read/write head **200** having a SOT device. The read/write head **200** faces a magnetic media **112**. The read/write head **200** may correspond to the magnetic head assembly **121** described in FIG. **1**. The read/write head **200** includes a media facing surface (MFS) **212**, such as a gas bearing surface, facing the disk **112**, a write head **210**, and a magnetic read head **211**. As shown in FIG. **2**, the magnetic media **112** moves past the write head **210** in the direction indicated by the arrow **232**, and the read/write head **200** moves in the direction indicated by the arrow **234**.

[0034] In some embodiments, the magnetic read head **211** is a magnetoresistive (MR) read head with an MR sensing element **204** located between MR shields S**1** and S**2**. In other embodiments, the magnetic read head **211** is a magnetic tunnel junction (MTJ) read head that includes an MTJ sensing device **204** disposed between MR shields S**1** and S**2**. The magnetic fields of the adjacent magnetized regions in the magnetic disk **112** are detectable by the MR (or MTJ) sensing element **204** as the recorded bits. The SOT device of various embodiments can be incorporated into the read head **211** as the sensing element. An example of a SOT read head is described in a co-pending patent application titled "Topological Insulator Based Spin Torque Oscillator Reader," U.S. application Ser. No. 17/828,226, filed May 31, 2022, assigned to the same assignee of this application, which is herein incorporated by reference. Another example of a SOT read head is described in co-pending patent applications titled "Non-Localized Spin Valve Reader Hybridized With Spin Orbit Torque Layer," U.S. application Ser. No. 18/367,877, filed Sep. 13, 2023, and "Non-Localized Spin Valve Multi-Free-Layer Reader Hybridized With Spin Orbit Torque Layers," U.S. application Ser. No. 18/367,882, filed Sep. 13, 2023, which is herein incorporated by reference.

[0035] The write head **210** includes a central or main pole **220**, a leading shield **206**, a trailing shield **240**, an optional spin-orbital torque (SOT) device **250**, and a coil **218** that excites the main pole **220**. The coil **218** may have a "pancake" structure that winds around a back-contact between the main pole **220** and the trailing shield **240**, instead of a "helical" structure shown in FIG. **2**. For example, when included, e.g., to achieve a Microwave Assisted Magnetic Recording (MAMR) effect, the SOT device **250** is formed in a gap **254** between the main pole **220** and the trailing shield **240**. The main pole **220** includes a trailing taper **242** and a leading taper **244**. The trailing taper **242** extends from a location recessed from the MFS **212** to the MFS **212**. The leading taper **244** extends from a location recessed from the MFS **212** to the MFS **212**. The trailing taper **242** and the leading taper **244** may have the same degree of taper, and the degree of taper is measured with respect to a longitudinal axis **260** of the main pole **220**. In some embodiments, the main pole **220** does not include the trailing taper **242** and the leading taper **244**. Instead, the main pole **220** includes a trailing side (not shown) and a leading side (not shown), and the trailing side and the leading side are substantially parallel. The main pole **220** may be a magnetic material, such as a FeCo alloy. The leading shield **206** and the trailing shield **240** may comprise magnetic materials, such as a NiFe alloy. In certain embodiments, the trailing shield **240** can include a trailing shield hot seed layer **241**. The trailing shield hot seed layer **241** can comprise a high moment sputter material, such as CoFeN, FeXN, or FeX, where X includes at least one of N, Al, Ni, Co, Ta, Re, Ir, Pt, Rh, Ta, Zr, and Ti. In certain embodiments, the trailing shield **240** does not include a trailing shield hot seed layer.

[0036] FIGS. **3**A-**3**B illustrate spin-orbit torque (SOT) devices **300**, **350**, according to various embodiments. The SOT devices **300** and **350** may be used individually in the MAMR recording head of the drive **100** of FIG. **1**, in the reader, and/or writer portions of the head **200** of FIG. **2**, or other suitable magnetic media drives. The SOT devices **300** and **350** may each individually be an MTJ in sensors or MRAM applications, such as the example MRAM embodiment disclosed in FIG. **7**, and spin-charge conversion layers/structures in logic circuits that can be used in artificial intelligence chips. Aspects of the SOT devices **300** and **350** may be used in combination with one another.

[0037] The SOT device **300** of FIG. **3**A comprises a seed layer **302**, a buffer layer **304** disposed over the seed layer **302**, a first migration barrier layer **306** disposed over the buffer layer **304**, a topological semi-metal (TSM) layer **312** disposed on the first migration barrier layer **306**, an interlayer **310** disposed on the TSM layer **312**, a ferromagnetic (FM) layer **316** disposed on the interlayer **310**, and a cap layer **318** disposed on the FM layer **316**. The interlayer **310** comprises a second migration barrier layer **308** disposed on the TSM layer **312** and a sub-interlayer **314** disposed on the second migration barrier layer **308**. The first migration barrier layer **306** may comprise a different material than the second migration barrier layer **308**. In some embodiments, the second migration barrier layer **308** and the sub-interlayer **314** are considered separate layers, rather than the interlayer **310**. The buffer layer **304** may have a (100) orientation, (111) orientation, or a (110) orientation. In some embodiments, the buffer layer **304** comprises the first migration barrier layer **306**.

[0038] The SOT device **350** of FIG. **3**B comprises the seed layer **302**, the FM layer **316** disposed on the seed layer **302**, the interlayer **310** disposed on the FM layer **316**, the TSM layer **312** disposed on the interlayer **310**, the first migration barrier layer**306** disposed on the TSM layer **312**, the buffer layer **304** disposed on the first migration barrier layer **306**, and the cap layer **318** disposed on the buffer layer **304**. The interlayer **310** comprises the sub-interlayer **314** disposed on the FM layer **316**, and the second migration barrier layer **308** disposed between the sub-interlayer **314** and the TSM layer **312**. The first migration barrier layer **306** may comprise a different material than the second migration barrier layer **308**. The sub-interlayer **314** may have a (100) orientation, a (110) orientation, or a (111) orientation. In some embodiments, the buffer layer **304** comprises the first migration barrier layer **306**.

[0039] In both SOT devices **300** and **350**, the first and second migration barrier layers **306** and **308** are disposed in contact with the TSM layer **312** such that the TSM layer **312** is sandwiched between the first and second migration barrier layers **306** and **308**. The buffer layer **304**, the interlayer **310**, and the cap layer **318** promote epitaxial crystal symmetry growth of the TSM layer **312** while minimizing shunting. The migration barrier layers **306** and **308** further transmit the epitaxial growth and, due to minimal chemical interaction, prevent diffusion of the TSM layer **312** out and prevent materials from diffusing into the TSM layer **312** from the buffer layer **304**, the interlayer **310**, and the cap layer **318**.

[0040] The TSM layer **312** comprises YPtBi having a (100) orientation or a (110) orientation. The YPtBi has a 1:1:1 stoichiometry, and a density of about 9.7 g/cc to about 11.2 g/cc, such as a density of about 11 g/cc or greater. The YPtBi of the TSM layer **312** may comprise trace, detectable amounts of Kr, such as about 1% or less of Kr. The TSM layer **312** comprising YPtBi having a 1:1:1 stoichiometry achieves the highest spin Hall angle during operation. The methods of achieving such a high density are described below in FIGS. **4**A-**5**B. The TSM layer **312** has a thickness in the y-direction of about 100 Å to about 140 Å, such as about 120 Å.

[0041] The first migration barrier layer **306** may comprise a different material than the second migration barrier layer **308**. The first and second migration barrier layers **306**, **308**, are not only effective at reducing elemental migration. Still, they are generally higher resistance layers that reduce electrical shunting between layers and serve to transfer the (100) or (110) epitaxial growth from one layer to the next, or to the topological SOT layers which lowers interfacial roughness. Barrier layers can be selected from 3 different nonmagnetic type material groups.

[0042] The first group of materials for the barrier layers **306** and **308** includes these options: (1) high lattice parameter, higher resistance, atomically ordered stoichiometric B**2** (AB) binary alloys, such as RuHf and Zr—X alloys, where X is one or more of Co, Cu, Ru, and Rh; (2) Ti—Y alloys, where Y is one or more of Au, Ru, and Rh; or (3) stoichiometric B2 ternary A (BxC1-x) alloys, like (HfTi).5Ru, Ru(AlV).5, (AlMo).5Ti, and CoZrX, where X is one or more of Ti, Fe, Ni, Nb, and Mo (examples include (Co (Ti.3Zr.7), (Co.8Fe.2)Zr, (CoNi).5Zr, Co (Nb.25Zr.75)). The barrier layers **306**, **308** can also be disordered nonstoichiometric binary, ternary, or higher bcc alloys where multiple elements are selected, to form a bcc alloy, from the group consisting of: Ta, Hf, W, Ir, Pt, Y, Zr, Nb, Mo, Mg, Sc, Ti, V, Cr, Fe, Co,

Ni, Cu, Ru, Rh, and Ag, where all have lattice parameters in the range of 2.87 Å to 3.38 Å.

[0043] The second group of materials for the barriers layers **306** and **308** are fcc materials with lattice parameters about 4.08 Å to 4.75 Å, such as oxides of Ti, Mg, Ni, Zn, or Zr; or X—N or X—C composites where X is one or more of Sc, Ti, V, Cr, Zr, Nb, Ta, Hf, and W, as well as alloy composites of the above.

[0044] The third group of materials for the barrier layers **306** and **308** are tetragonal oxides with a-axis lattice parameters in a range of 4.35 Å to 4.75 Å and c-axis in the range of 2.85 Å to 3.19 Å, like MO_2 materials, examples of which include where M is Ti, Cr, Ru, Rh, Sn, Sb, or Ir; or CrNb, CrV, and WV alloys; or any combination thereof.

[0045] The first two barrier layer material groups can be used with either (100) or (110) texturing layers to form (100) or (110) textured barrier layers **306**, **308**. The texturing of the third group of barrier layer materials (i.e., the MO_2 tetragonal oxides) will depend on the texturing layer type. For (100) texturing layers, the MO_2 tetragonal oxides will produce (001) textured MO_2 tetragonal oxides, which in turn can be used to create (100) texture in other layers. With (110) texturing layers, the MO_2 tetragonal oxides will create a (110) textured tetragonal $M0_2$ oxide layer, but only for oxides where the a/c ratio is near the sqrt(2), such as where M is Os, Ir, Ru, Rh, or Pd. The first migration barrier layer **306** may comprise a different material than the second migration barrier layer **308**. Each barrier layer **306** and **308** may comprise one or more barrier layers depending on the application to optimize growth, electrical shunting, or elemental migration properties between layers.

[0046] The seed layer **302** comprises an amorphous or nanocrystalline material. The seed layer **302** may comprise a laminated structure comprising one or more materials selected from the group consisting of NiTa, RuAl, MgO, MgTiO, CrMo, CoFeTa, NiFeGe, NiFeTa, NiW, Ru, IrAl, and combinations thereof. The seed layer **302** has a thickness in the y-direction of about 10 Å to about 30 Å, such as about 20 Å.

[0047] The buffer layer **304** may comprise a combination of materials selected from the groups consisting of (100) or (110) textured layers, or mixtures thereof, with the groups of (a)-(k) listed below: (a) bcc metals or alloys with a-axis lattice parameters in the range of 2.9 Å to about 3.4 Å, such as Ta, W, Mo, Nb, WTi, and CrMo; (b) B2 metals with the same lattice parameter range, such as binary alloys of RuAl, RuHf, Zr—X alloys, where X is one or more of Co, Cu, Ru, and Rh, or Ti—Y alloys where Y is one or more of Au, Ru, and Rh; (c) B2 ternary alloys like HfRuTi, RuAlV, AlTiMo, and CoZrX, where X is one or more of Ti, Fe, Ni, Nb, and Mo, or any combinations of the above; (d) (100) and (110) textured fcc materials with lattice parameters about 4.08 Å to about 4.75 Å, such as oxides of Ti, Mg, Ni, Zn, and Zr, X—N, or X—C composites, where X is one or more of Sc, Ti, V, Cr, Zr, Nb, Ta, Hf, and W, as well as alloy composites of the above; (e) (001) textured tetragonal oxides with a-axis lattice parameters in a similar range as above, such as MO_2 materials, where M is one or more of Ti, Cr, Ru, Rh, Sn, Sb, and Ir, or alloy composites thereof; (f) (110) textured tetragonal MO_2 where a/c ratio is near the sqrt(2), such as where M is one or more of Os, Ir, Ru, Rh, Sn, Sb, and Pd; (g) high lattice parameter fcc (110) or (100) textured Heusler alloys, either half metallic or full, with lattice parameters in the range of 5.9 Å to 6.7 Å, such as MnSbPt (6.20 Å) or Sc_2VGe (a=6.65 Å), and Pd_2SnY (6.70 Å); (h) other spinel cubic materials with the space group **216** and similar lattice parameters, such as YNiBi, YPdBi, NiBiGd, AgMgSb, and BiXPt (where X is a rare earth element from Gd to Lu); (i) (100) textured layer materials such as X—Al, where X is one or more of Co, Ni, Ru, Rh, and Ir; (j) heated Cr or CrX alloys, where X is one or more of Mo, Mn, Ti, Ru, and W; and (k) combinations thereof.

[0048] Those skilled in the art can grow bcc metals along the close-packed direction creating strong (110) textured bcc or bcc alloy films mentioned above with lattice parameters in the range of 2.9 Å to 3.4 Å range, using combinations of nanocrystalline conditioning layers and other bcc seed layer materials; alloys seed layer films, such as the Cr—X alloys mentioned above; or by using thin (001) hcp Ru seeds. These highly textured (110) bcc or bcc alloy films can then be used to grow fcc (110) textured buffer layer films with lattice parameters of about 4.08 Å to 4.75 Å mentioned; (110) textured binary or ternary or higher B2 alloys mentioned above; or high lattice parameter fcc Heuslers or spinels with lattice parameters in the range of about 5.9 Å to 6.7 Å mentioned above, which can be utilized as high resistance or migration buffers layers on which to grow (110) textured YPtBi SOT layers. (110) textured buffer layers of MO_2 oxides could also be used for those oxides that have a/c ratios near the sqrt (2), as mentioned above.

[0049] Those skilled in the art can also grow bcc metals or B2 materials and alloys with a strong (100) texture and lattice parameters in the range of about 2.9 Å to 3.4 Å, like those of RuAl or heated Cr—X alloys mentioned above. These (100) textured layers can be used to grow strong fcc (100) textured buffer layers with lattice parameters in the range of 4.08 Å to 4.75 Å mentioned above; (100) textured Heusler alloys or spinel-type structures with lattice parameters in the range of 5.9 Å to 6.75 Å mentioned above; or (001) textured MO2 tetragonal oxides mentioned above with axis lattice parameters in the 4.1 Å to 4.75 Å range.

[0050] Buffer layers between the textured seed layers and the SOT layer can, in general, offer better control of electrical shunting between the seed layers and the SOT layer, or serve as migration barriers to prevent intermixing of the SOT layer and seed layers, or provide better film epitaxial growth to the YPtBi or BiSbX SOT layer.

[0051] The FM layer **316** has a thickness of about 5 Å to about 15 Å and may comprise NiFe, CoFe, NiFeX, CoFex, Fex, or Nix, where X is one or more of Co, Ni, Cu, Si, Al, Mn, Ge, Ta, Hf, N, or B. The FM layer **316** may comprise any magnetic layer combination or alloy combination of these elements that can yield a low coercivity, negative magnetostrictive FM layer **316**, or in multilayer combinations with other higher polarizing materials like Heusler alloys or high Ni-containing alloy FM layers. The sub-interlayer **314** may comprise MgO, CoFeB, Co, CoFe, NiFe, or a similar material as the FM layer **316**. The sub-interlayer **314** and the interlayer **310** collectively have a thickness in the y-direction of about 20 Å or less.

[0052] The cap layer **318** may comprise nonmagnetic, high resistivity materials, such as: thin ceramic oxides or nitrides of TIN, SiN, MgTiO, and MgO; amorphous/nanocrystalline metals such as NiFeGe, NiFeTa, NiTa, NiHf, NiFeHf, CoHf, CoFeHf, NiWTa, NiFeW, NiW, WRe; or nitrides, oxides, or borides of elements as mentioned earlier, compounds, and/or alloys such as NiTaN, NiFeTaN, NiWTaN, NiWN, WREN, TaN, WN, TaOx, WOx, WB,

HfB, NiHfB, NiFeHfB, CoHfB, and CoFeHfB, where x is a numeral. In some embodiments, lower atomic number (Z) materials are preferred in the cap layer **318** to reduce sputter intermixing with the FM layer **316**. High Z alloys can be used, if combined with a migration barrier beneath, or if the high Z elements are used with a high resistive oxide, nitride, or boride. The cap layer **318** can comprise multilayer combinations of the materials as mentioned earlier, and the overall thickness of the cap layer **318** is less than or equal to about 100 Å (nominally about 15 Å to about 50 Å).

[0053] FIGS. **4**A-**4**C illustrate methods **400**, **430**, and **450**, respectively, of forming YPtBi having a 1:1:1 composition, according to various embodiments. The methods **400**, **430**, and **450** may each be used to create the TSM layer **312** or FIGS. **3**A-**3**B.

[0054] In the method **400** of FIG. **4**A, at block **402**, a substrate is loaded onto a chuck heated to a temperature of about 300° C. to about 600° C. in a deposition chamber. The deposition chamber may be any known deposition chamber, such as a physical vapor deposition (PVD) chamber.

[0055] At block **404**, one of the following target combinations is placed in the deposition chamber: 1) a YPt target and a Bi target; 2) a YBi target and a Bi target; or 3) PtBi target and a Y target. The targets may not be 50/50 targets due to preferential sputtering of Bi. As such, the targets may contain less Bi than about 50%. At block **406**, the Kr, Ar, or Xe gas flow, pressure, and substrate bias within the deposition chamber are adjusted. The Kr, Ar, or Xe gas flow may be about 25 sccm to about 55 sccm, such as about 40 sccm. The pressure may be about 0.2 mtorr to about 20 mtorr, or about 0.2 mtorr or less, while holding a stable plasma. The substrate bias may be about 20 V to about 200 V, such as about 50 V±25 V.

[0056] At block **408**, power and Kr, Ar, or Xe gas are applied to the selected targets to sputter the targets on the substrate to form a film comprising YPtBi having a 1:1:1 stoichiometry or composition. Different power levels may be applied to each target when sputtering. For example, when a YPt target and a Bi target are selected, a first power of about 90 W to about 200 W may be used when sputtering the YPt target, and a second power of about 20 W to about 50 W may be used when sputtering the Bi target. In some embodiments, the power applied to the Bi target is about 20% to about 30% of the power applied to the YPt target, or a ratio of about 5:1 for the YPt target to the Bi target.

[0057] Utilizing different power levels, and adjusting the Kr, Ar, or Xe gas flow, enables the YPtBi film to achieve a 1:1:1 stoichiometry and a high density between about 9.7 g/cc to about 11.2 g/cc. In some embodiments, the density of the YPtBi film is greater than about 11 g/cc. Moreover, trace amounts of Kr are detectable in the completed film. For example, about 0.5 at. % to about 2.0 at. % of Kr, Ar, or Xe may be detectable as a dopant.

[0058] In the method **430** of FIG. **4**B, at block **432**, a substrate is loaded onto a chuck heated to a temperature of about 300° C. to about 600° C. in a deposition chamber. The deposition chamber may be any known deposition chamber, such as a physical vapor deposition (PVD) chamber.

[0059] At block **434**, a Y target, a Pt target, and a Bi target are placed in the deposition chamber. At block **436**, the gas flow, pressure, and substrate bias within the deposition chamber are adjusted. The gas flow may be about 25 sccm to about 55 sccm, such as about 40 sccm. The pressure may be about 0.2 mtorr to about 20 mtorr, or about 0.2 mtorr or less, while holding a stable plasma. The substrate bias may be about 20 V to about 200 V, such as about 50 V±25 V. At block **438**, power and Kr, Ar, or Xe gas are applied to the Y, Pt, and Bi targets to sputter the targets on the substrate to form a film comprising YPtBi having a 1:1:1 stoichiometry or composition. Different power levels may be applied to each target when sputtering. For example, a first power of about 100 W to about 500 W, such as about 115 W to about 125 W, may be used when sputtering the Y target, a second power of about 20 W to about 300 W, such as about 25 W to about 30 W when sputtering the Bi target, and a third power of about 20 W to about 500 W may be used when sputtering the Pt target. In some embodiments, the power applied to the Pt target is about 20% to about 30% of the power applied to the YBi target.

[0060] Utilizing different power levels, and adjusting the Kr, Ar, or Xe gas flow, enables the YPtBi film to achieve a 1:1:1 stoichiometry and a high density between about 9.7 g/cc to about 11.2 g/cc. In some embodiments, the density of the YPtBi film is greater than about 11 g/cc. Moreover, trace amounts of Kr are detectable in the completed film. For example, about 0.1 at. % to about 2.5 at. % of Kr, Ar, or Xe may be detectable as a dopant.

[0061] In the method **450** of FIG. **4**C, at block **452**, a substrate is loaded onto a chuck heated to a temperature of about 300° C. to about 600° C. in a deposition chamber. The deposition chamber may be any known deposition chamber, such as a physical vapor deposition (PVD) chamber.

[0062] At block **454**, a YPtBi target is placed in the deposition chamber. For example, to form the YPtBi target, the following amounts may be used: about 10 grams (g) to about 15 g of Y, about 20 g to about 30 g of Pt, and about 20 g to about 40 g of Bi. At block **456**, the gas flow, pressure, and substrate bias within the deposition chamber are adjusted. The gas flow may be about 25 sccm to about 55 sccm, such as about 40 sccm. The pressure may be about 0.2 mtorr to about 20 mtorr, or about 0.2 mtorr or less, while holding a stable plasma. The substrate bias may be about 20 V to about 200 V, such as about 50 V±25 V.

[0063] At block **458**, power and Kr, Ar, or Xe gas are applied to the YPtBi target to sputter the targets on the substrate to form a film comprising YPtBi having a 1:1:1 stoichiometry or composition. The power applied to the YPtBi target may be about 20 W to about 500 W. Adjusting the power level and the gas flow enables the YPtBi film to achieve a 1:1:1 stoichiometry and a high density between about 9.7 g/cc to about 11.2 g/cc. In some embodiments, the density of the YPtBi film is greater than about 11 g/cc. Moreover, trace amounts of Kr, Ar, or Xe are detectable in the completed film. For example, about 0.1 at. % to about 2.5 at. % of Kr, Ar, or Xe may be detectable as a dopant.

[0064] FIG. **5**A illustrates a graph **500** showing that, in order to read a 1:1:1 composition, the power ratio between the power (W) applied to the Bi target versus the power (W) applied to the YPt target is fixed, according to one embodiment. FIG. **5**B illustrates a graph **550** showing the stoichiometry of YPt difference between Pt and Y in a sputtered YPtBi film is controlled by the Kr gas flow (sccm), according to one embodiment. While the graphs **500** and **550** correspond to the method **400** of FIG. **4**A using a YPt target and a Bi target, the graphs are merely intended to be examples, and may apply to the methods **430** and **450** of FIGS. **4**B-**4**C. Kr gas is used as an example, but the gas may be Ar or Xe as well.

[0065] As shown in the graphs **500** and **550**, when a YPtBi film is deposited at a Kr gas flow of about 40 sccm and a power of about 20 W to about 45 W is applied to the Bi target, and a power of about 90 W to about 200 W is applied to the YPt (50/50) target, the resulting YPtBi having a 1:1:1 stoichiometry achieves a high density between about 9.7 g/cc to about 11.2 g/cc.

[0066] Also shown in the graph **550**, a 1:1 relative Y to Pt stoichiometry is achieved in a YPtBi film for a non-stoichiometry YPt (49/51) target (a ±2% delta) when the Kr gas flow is between about 15 sccm to about 55 sccm, such as about 15 sccm, when the powers of Bi and YPt from the graph **500** are applied to Bi and YPt targets, respectively.

[0067] FIG. **6**A is a schematic cross-sectional view of a SOT device **600** for use in a MAMR magnetic recording head, such as the MAMR magnetic recording head of the drive **100** of FIG. **1** or other suitable magnetic media drives. The SOT device **600** comprises a TSM layer **312** orientation formed over a buffer layer **304** formed over a substrate **601**, such as the TSM layer **312** and the buffer layer **304** of FIG. **3**A or the TSM layer **312** and the buffer layer **304** of FIG. **3**B. Thus, the TSM layer **312** may comprise YPtBi having a (100) orientation or YPtBi having a (110) orientation. A spin torque layer (STL) **670** is formed over the TSM layer **312**. The STL **670** comprises a ferromagnetic material such as one or more layers of CoFe, CoIr, NiFe, and CoFeX alloy wherein X═B, Ta, Re, or Ir.

[0068] In certain embodiments, an electrical current shunt block layer **660** is disposed between the TSM layer **312** and the STL **670**. The electrical current shunt blocking layer **660** reduces electrical current from flowing from the TSM layer **312** to the STL **670** but allows spin orbital coupling of the TSM layer **312** and the STL **670**. In certain embodiments, the electrical current shunt blocking layer **660** comprises a magnetic material that provides greater spin orbital coupling between the TSM layer **312** and the STL **670** than a nonmagnetic material. In certain embodiments, the electrical current shunt blocking layer **660** comprises a magnetic material of FeCo, FeCOM, FeCOMO, FeCoMMeO, FeCOM/MeO stack, FeCoMNiMnMgZnFeO, FeCOM/NiMnMgZnFeO stack, multiple layers/stacks thereof, or combinations thereof in which M is one or more of B, Si, P, Al, Hf, Zr, Nb, Ti, Ta, Mo, Mg, Y, Cu, Cr, and Ni. Me is one or more of Si, Al, Hf, Zr, Nb, Ti, Ta, Mg, Y, or Cr. In certain embodiments, the electrical current shunt blocking layer **660** is formed to a thickness from about 10 Å to about 100 Å. In certain aspects, an electrical current shunt blocking layer **660** with a thickness of over 100 Å may reduce the spin-orbital coupling of the TSM layer **312** and the STL **670**. In certain aspects, an electrical current shunt blocking layer having a thickness of less than 10 Å may not sufficiently reduce electrical current from TSM layer **312** to the STL **670**.

[0069] In certain embodiments, additional layers are formed over the STL **670** such as a spacer layer **680** and a pinning layer **690**. The pinning layer **690** can partially pin the STL **670**. The pinning layer **690** comprises a single or multiple layers of PtMn, NiMn, IrMn, IrMnCr, CrMnPt, FeMn, other antiferromagnetic materials, or combinations thereof. The spacer layer **580** comprises single or multiple layers of magnesium oxide, aluminum oxide, other nonmagnetic materials, or combinations thereof.

[0070] FIGS. **6**B-**6**C are schematic MFS views of certain embodiments of a portion of a MAMR magnetic recording head **210** with a SOT device **600** of FIG. **6**A. The MAMR magnetic recording head **210** can be the magnetic recording head FIG. **2** or other suitable magnetic recording heads in the drive **100** of FIG. **1** or other suitable magnetic media drives such as tape drives. The MAMR magnetic recording head **210** includes a main pole **220** and a trailing shield **240** in a track direction. The SOT device **600** is disposed in a gap between the main pole and the trailing shield **240**.

[0071] While the MRAM device **600** generally corresponds to the top-SOT embodiments of FIG. **3**B, other MRAM implementations (where the layers of MRAM device **600** are reversed) can correspond or conform to the bottom-SOT embodiments of FIG. **3**A. The TSM layer **312**, the RL **610**, and the buffer layer **302** in FIG. **6** may correspond to various layer configurations in FIGS. **3**A-**3**B. For example, the TSM layer **312** can correspond to the TSM layer **312**. Thus, the TSM layer **312** may comprise YPtBi having a (100) orientation or YPtBi having a (110) orientation. The RL **610** may correspond to the FM layer **316**. The buffer layer **304** may correspond to the buffer layer **304**.

[0072] During operation, charge current through a TI layer or layer stack **312** acting as a spin Hall layer generates a spin current in the BiSb layer. The spin orbital coupling of the BiSb layer and a spin torque layer (STL) **670** causes switching or precession of magnetization of the STL **670** by the spin orbital coupling of the spin current from the TSM layer **312**. Switching or precession of the magnetization of the STL **670** can generate an assisting AC field to the write field. Energy-assisted magnetic recording heads based on SOT have multiple times greater power efficiency than MAMR magnetic recording heads based on spin transfer torque. As shown in FIG. **6**B, an easy axis of a magnetization direction of the STL **670** is perpendicular to the MFS from shape anisotropy of the STL **670**, from the pinning layer **690** of FIG. **6**A, and/or from hard bias elements proximate to the STL **670**. As shown in FIG. **6**C, an easy axis of a magnetization direction of the STL **670** is parallel to the MFS from shape anisotropy of the STL **670**, from the pinning layer **690** of FIG. **6**A, and/or from complex bias elements proximate to the STL **670**.

[0073] FIG. **7** is a schematic cross-sectional view of an SOT MTJ **701** used as a MRAM device **700**. The MRAM device **700** comprises a reference layer (RL) **710**, a spacer layer **720** over the RL **710**, a recording layer **730** over the spacer layer **720**, a buffer layer **704** over an electrical current shunt block layer **740** over the recording layer **630**, and a TI layer or layer stack **312** over the buffer layer **304**. The TSM layer **312** and the buffer layer **304** may be the TSM layer **312** and the buffer layer **304** of FIG. **3**A or the TI layer **332** and the buffer layer **360** of FIG. **3**B. Thus, the TSM layer **312** may comprise YPtBi having a (100) orientation or YPtBi having a (110) orientation.

[0074] The RL **710** comprises single or multiple layers of CoFe, other ferromagnetic materials, and combinations thereof. The spacer layer **720** comprises single or multiple layers of magnesium oxide, aluminum oxide, other dielectric materials, or combinations thereof. The recording layer **730** comprises single or multiple layers of CoFe, NiFe, other ferromagnetic materials, or combinations thereof.

[0075] As noted above, in certain embodiments, the electrical current shunt block layer **740** is disposed between the buffer layer **304** and the recording layer **730**. The electrical current shunt blocking layer **740** reduces electrical current from flowing from the TSM layer **312** to the recording layer

730. The electrical current shunt blocking layer **740** still allows spin orbital coupling of the TSM layer **312** and the recording layer **730**. For example, writing to the MRAM device can be enabled by the spin orbital coupling of the TSM layer and the recording layer **730**, which allows switching of magnetization of the recording layer **730** by the spin orbital coupling of the spin current from the TSM layer **312**. In certain embodiments, the electrical current shunt blocking layer **740** comprises a magnetic material that provides greater spin orbital coupling between the TSM layer **312** and the recording layer **730** than a nonmagnetic material. In certain embodiments, the electrical current shunt blocking layer **740** comprises a magnetic material of FeCOM, FeCOMO, FeCOMMeO, FeCOM/MeO stack, FeCOMNiMnMgZnFeO, FeCOM/NiMnMgZnFeO stack, multiple layers/stacks thereof, or combinations thereof, in which M is one or more of B, Si, P, Al, Hf, Zr, Nb, Ti, Ta, Mo, Mg, Y, Cu, Cr, and Ni; and Me is Si, Al, Hf, Zr, Nb, Ti, Ta, Mg, Y, or Cr.

[0076] The MRAM device **700** of FIG. **7** may include other layers, such as pinning layers, pinning structures (e.g., a synthetic antiferromagnetic (SAF) pinned structure), electrodes, gates, and other structures. Other MRAM devices besides the structure of FIG. **6** can be formed utilizing a TSM layer **312** over a buffer layer **304** to form a SOT MTJ **701**.

[0077] Therefore, high spin Hall angles can be achieved by utilizing a YPtBi film having a 1:1:1 stoichiometry and a high density of about 9.7 g/cc to about 11.2 g/cc in an SOT device.

[0078] In other embodiments, the TSM layer **312** of the SOT devices **300** and **350** comprises YPtBi having a 1:1.02:1.05 stoichiometry to a 1:1.25:1.35 stoichiometry, such as about a 1:1.11:1.13 stoichiometry. In other words, the atomic concentration of Pt and Bi are nearly the same as one another, while Y is deficient by 10% compared with Pt and Bi. The concentrations of Pt and Bi in YPtBi affect both the effective spin Hall angle (θ_{SH}^{eff}) and the effective spin Hall conductivity (σ_{SH}^{eff}). By increasing the concentration of Pt in YPtBi, the grain size of the TSM layer **312** changes, improving the spin current though the SOT devices **300**, **350**. By increasing the concentration of Bi in YPtBi to approach that of Pt, defects are removed from the TSM layer **312**, resulting in higher resistivity and a higher spin Hall angle.

[0079] FIG. **8**A illustrates a graph **800** showing how the conductivity (σ_{YPtBi}) of the TSM layer **312** is impacted when the composition ratio of Pt to Y (Pt/Y) in YPtBi is increased, according to one embodiment. FIG. **8**B illustrates a graph **825** showing how the effective spin Hall angle is impacted when the composition ratio of Pt to Y (Pt/Y) in YPtBi is increased, according to one embodiment. FIG. **8**C illustrates a graph **850** showing how the effective spin Hall conductivity (σ_{SH}^{eff}) is impacted when the composition ratio of Pt to Y (Pt/Y) in YPtBi is increased, according to one embodiment, where x represents multiplication, e is the electron charge, and $\hbar$ is the Dirac constant. In the graphs **800**, **825**, **850**, the concentration ratio of Y to Pt is 1.

[0080] As shown in the graphs **825** and **850**, increasing the Pt/Y atomic concentration ratio from 1.02 to 1.11 enhances both the spin Hall angle and the spin Hall conductivity by a factor of two. Thus, increasing Pt atomic concentration helps increase the YPtBi surface grain size, which in turn helps improve the interface spin transparency.

[0081] FIG. **8**D illustrates a graph **875** showing how the conductivity (σ_{YPtBi}) of the TSM layer **312** is impacted when the composition ratio of Bi to Y (Bi/Y) in YPtBi is increased, according to one embodiment. FIG. **8**E illustrates a graph **885** showing how the effective spin Hall angle is impacted when the composition ratio of Bi to Y (Bi/Y) in YPtBi is increased, according to another embodiment. FIG. **8**F illustrates a graph **895** showing how the effective spin Hall conductivity (σ_{SH}^{eff}) is impacted when the composition ratio of Bi to Y (Bi/Y) in YPtBi is increased, according to another embodiment. In the graphs **875**, **885**, **895**, the concentration ratio of Y to Bi is 1.

[0082] As shown in the graphs **875**, **885**, **895**, the conductivity of the YPtBi and the effective spin Hall angle (θ_{SH}^{eff}) are influenced by the Bi ratio, but the effective spin Hall conductivity (σ_{SH}^{eff}) is largely unchanged. Thus, increasing the Bi concentration ratio affects the conductivity of the TSM layer **312**, which in turn affects the effective spin Hall angle.

[0083] Therefore, an SOT device comprising a TSM layer of YPtBi having a 1:1.02:1.05 stoichiometry to a 1:1.25:1.35 stoichiometry, such as about a 1:1.11:1.13 stoichiometry, increases the spin Hall angle and the spin Hall conductivity. Increasing Pt atomic concentration to greater than 1 enhances both the spin Hall angle and the spin Hall conductivity by a factor of two, and further helps increase the YPtBi surface grain size, which in turn helps improve the interface spin transparency. Increasing the Bi/Y atomic concentration ratio to greater than **1**, approaching that of Pt, reduces the defects, thus enhancing both the resistivity of the YPtBi layer and the effective spin Hall angle (θ_{SH}^{eff}) by a factor of two.

[0084] In one embodiment, a spin-orbit torque (SOT) device comprises a YPtBi layer having a 1:1.02:1.05 stoichiometry to a 1:1.25:1.35 stoichiometry.

[0085] Various embodiments may include the following options or configurations. The YPtBi layer has a 1:1.11:1.13 stoichiometry. The YPtBi layer has a (100), (111), or (110) orientation. The SOT device further comprises a buffer layer disposed adjacent to the YPtBi layer. The buffer layer comprises a material selected from the group consisting of: X—Al, where X is one or more of Co, Ni, Ru, Rh, and Ir; Cr or CrX alloys, where X is one or more of Mo, Mn, Ti, Ru, and W; and RuAl, W—X, or Ta—X alloys with MgO and TiO, where X is one or more of Ta, Hf, W, V, Ti, Nb and Mo. The buffer layer comprises a material selected from the group consisting of: RuHf; Zr—X alloys, where X is one or more of Co, Cu, Ru, and Rh; Ti—Y alloys, where Y is one or more of Au, Ru, and Rh; B2 ternary A (BxC1-x) alloys; B2 binary alloys; CoZrX, where X is one or more of Ti, Fe, Ni, Nb, and Mo; two or more elements selected from the group consisting of: Ta, Hf, W, Ir, Pt, Y, Zr, Nb, Mo, Mg, Sc, Ti, V, Cr, Fe, Co, Ni, Cu, Ru, Rh, and Ag; oxides of Ti, Mg, Ni, Zn, or Zr; X—N or X—C composites, where X is one or more of Sc, Ti, V, Cr, Zr, Nb, Ta, Hf, and W; and MO_2 materials, where M is one or more of Ti, Cr, Ru, Rh, Sn, Sb, Ir, CrNb, CrV, and WV. A magnetic recording head comprises the SOT device. A magnetic recording device comprises the magnetic recording head. A magnetoresistive memory comprises the SOT device.

[0086] In another embodiment, a spin-orbit torque (SOT) device comprises a YPtBi layer, wherein a concentration of Pt and Bi is about 10% greater than a concentration of Y.

[0087] Various embodiments may include the following options or configurations. The YPtBi layer has a 1:1.02:1.05 stoichiometry to a 1:1.25:1.35 stoichiometry. The YPtBi layer has a 1:1.11:1.13 stoichiometry. The YPtBi layer has a (100), (111), or (110) orientation. A magnetic recording head comprises the SOT device. A magnetic recording device comprises the magnetic recording head. A magnetoresistive memory comprises the SOT device.

[0088] In yet another embodiment, a spin-orbit torque (SOT) device comprises a YPtBi layer having a 1:1.02:1.05 stoichiometry to a 1:1.25:1.35 stoichiometry, wherein the YPtBi layer has a (100), (111), or (110) orientation, and a buffer layer disposed adjacent to the YPtBi layer.

[0089] Various embodiments may include the following options or configurations. The YPtBi layer has a 1:1.11:1.13 stoichiometry. The buffer layer comprises a material selected from the group consisting of: X—Al, where X is one or more of Co, Ni, Ru, Rh, and Ir; Cr or CrX alloys, where X is one or more of Mo, Mn, Ti, Ru, and W; and RuAl, W—X, or Ta—X alloys with MgO and TiO, where X is one or more of Ta, Hf, W, V, Ti, Nb and Mo. The buffer layer comprises a material selected from the group consisting of: RuHf; Zr—X alloys, where X is one or more of Co, Cu, Ru, and Rh; Ti—Y alloys, where Y is one or more of Au, Ru, and Rh; B2 ternary A (BxC1-x) alloys; B2 binary alloys; CoZrX, where X is one or more of Ti, Fe, Ni, Nb, and Mo; two or more elements selected from the group consisting of: Ta, Hf, W, Ir, Pt, Y, Zr, Nb, Mo, Mg, Sc, Ti, V, Cr, Fe, Co, Ni, Cu, Ru, Rh, and Ag; oxides of Ti, Mg, Ni, Zn, or Zr; X—N or X—C composites, where X is one or more of Sc, Ti, V, Cr, Zr, Nb, Ta, Hf, and W; and MO_2 materials, where M is one or more of Ti, Cr, Ru, Rh, Sn, Sb, Ir, CrNb, CrV, and WV. A magnetic recording head comprises the SOT device. A magnetic recording device comprises the magnetic recording head. A magnetoresistive memory comprises the SOT device.

[0090] While the preceding is directed to embodiments of the present disclosure, other and further embodiments of the disclosure may be devised without departing from the basic scope thereof, and the scope thereof is determined by the following claims.

What is claimed is:

1. A spin-orbit torque (SOT) device, comprising:
a YPtBi layer having a 1:1.02:1.05 stoichiometry to a 1:1.25:1.35 stoichiometry.

2. The SOT device of claim **1**, wherein the YPtBi layer has a 1:1.11:1.13 stoichiometry.

3. The SOT device of claim **1**, wherein the YPtBi layer has a (100), (111), or (110) orientation.

4. The SOT device of claim **1**, further comprising a buffer layer disposed adjacent to the YPtBi layer.

5. The SOT device of claim **4**, wherein the buffer layer comprises a material selected from the group consisting of:
X—Al, where X is one or more of Co, Ni, Ru, Rh, and Ir;
Cr or CrX alloys, where X is one or more of Mo, Mn, Ti, Ru, and W; and
RuAl, W—X, or Ta—X alloys with MgO and TiO, where X is one or more of Ta, Hf, W, V, Ti, Nb and Mo.

6. The SOT device of claim **4**, wherein the buffer layer comprises a material selected from the group consisting of:
RuHf;
Zr—X alloys, where X is one or more of Co, Cu, Ru, and Rh;
Ti—Y alloys, where Y is one or more of Au, Ru, and Rh;
B2 ternary A (BxC1-x) alloys;
B2 binary alloys;
CoZrX, where X is one or more of Ti, Fe, Ni, Nb, and Mo;
two or more elements selected from the group consisting of: Ta, Hf, W, Ir, Pt, Y, Zr, Nb, Mo, Mg, Sc, Ti, V, Cr, Fe, Co, Ni, Cu, Ru, Rh, and Ag;
oxides of Ti, Mg, Ni, Zn, or Zr;
X—N or X—C composites, where X is one or more of Sc, Ti, V, Cr, Zr, Nb, Ta, Hf, and W; and
MO_2 materials, where M is one or more of Ti, Cr, Ru, Rh, Sn, Sb, Ir, CrNb, CrV, and WV.

7. A magnetic recording head comprising the SOT device of claim **1**.

8. A magnetic recording device comprising the magnetic recording head of claim **7**.

9. A magnetoresistive memory comprising the SOT device of claim **1**.

10. A spin-orbit torque (SOT) device, comprising:
a YPtBi layer, wherein a concentration of Pt and Bi is about 10% greater than a concentration of Y.

11. The SOT device of claim **10**, wherein the YPtBi layer has a 1:1.02:1.05 stoichiometry to a 1:1.25:1.35 stoichiometry.

12. The SOT device of claim **11**, wherein the YPtBi layer has a 1:1.11:1.13 stoichiometry.

13. The SOT device of claim **10**, wherein the YPtBi layer has a (100), (111), or (110) orientation.

14. A magnetic recording head comprising the SOT device of claim **10**.

15. A magnetic recording device comprising the magnetic recording head of claim **14**.

16. A magnetoresistive memory comprising the SOT device of claim **10**.

17. A spin-orbit torque (SOT) device, comprising:
a YPtBi layer having a 1:1.02:1.05 stoichiometry to a 1:1.25:1.35 stoichiometry, wherein the YPtBi layer has a (100), (111), or (110) orientation; and
a buffer layer disposed adjacent to the YPtBi layer.

18. The SOT device of claim **17**, wherein the YPtBi layer has a 1:1.11:1.13 stoichiometry.

19. The SOT device of claim **17**, wherein the buffer layer comprises a material selected from the group consisting of:
X—Al, where X is one or more of Co, Ni, Ru, Rh, and Ir;
Cr or CrX alloys, where X is one or more of Mo, Mn, Ti, Ru, and W; and
RuAl, W—X, or Ta—X alloys with MgO and TiO, where X is one or more of Ta, Hf, W, V, Ti, Nb and Mo.

20. The SOT device of claim **17**, wherein the buffer layer comprises a material selected from the group consisting of:
RuHf;
Zr—X alloys, where X is one or more of Co, Cu, Ru, and Rh;
Ti—Y alloys, where Y is one or more of Au, Ru, and Rh;
B2 ternary A (BxC1-x) alloys;
B2 binary alloys;
CoZrx, where X is one or more of Ti, Fe, Ni, Nb, and Mo;
two or more elements selected from the group consisting of: Ta, Hf, W, Ir, Pt, Y, Zr, Nb, Mo, Mg, Sc, Ti, V, Cr, Fe, Co, Ni, Cu, Ru, Rh, and Ag;
oxides of Ti, Mg, Ni, Zn, or Zr;
X—N or X—C composites, where X is one or more of Sc, Ti, V, Cr, Zr, Nb, Ta, Hf, and W; and
MO_2 materials, where M is one or more of Ti, Cr, Ru, Rh, Sn, Sb, Ir, CrNb, CrV, and WV.

21. A magnetic recording head comprising the SOT device of claim **17**.

22. A magnetic recording device comprising the magnetic recording head of claim **21**.

23. A magnetoresistive memory comprising the SOT device of claim **17**.

* * * * *